



TECHNICAL UNIVERSITY OF CRETE
SCHOOL OF MINERAL RESOURCES ENGINEERING
PETROLEUM ENGINEERING MASTER COURSE

Master Thesis

**“PERFORMANCE COMPARISON BETWEEN VARIOUS COMMERCIAL
SIMULATORS”**

Author:

Aleksandar Mirkovic

Supervisor: Prof. Nikolaos Varotsis

Examination Committee:

Prof. Nikolaos Varotsis

Prof. Vassilis Gaganis

Prof. Nikolaos Pasadakis

Chania, 2018

*A thesis submitted in fulfillment of the requirements for the
Master degree of Petroleum Engineering in the
School of Mineral Resources Engineering
Technical University of Crete*

*The MSc Program in Petroleum Engineering of the
Technical University of Crete, was attended and completed
by Mr. Aleksandar Mirkovic, due to the Hellenic Petroleum Group Scholarship award.*

Table of Contents

Table of Contents	iv
List of Figures	vi
List of Tables	vi
Acknowledgements	viii
Abstract	ix
1. The Function and Scope of Reservoir simulation.....	1
1.1 Introduction	1
1.2 Modeling approaches	1
1.2.1 Analogical methods	1
1.2.2 Experimental methods	2
1.2.3 Mathematical methods	2
1.3 Application of Reservoir Simulation.....	4
1.4 Reservoir simulators classification.....	6
2. Model building.....	7
2.1 Geological model	7
2.2 Flow models	9
2.3 Well models.....	13
3. Numerical methods in reservoir simulation.....	15
3.1 Review of finite difference.....	15
3.2 Application of finite difference on flow equation.....	17
3.2.1 Explicit finite difference approximation of the linear pressure equation	17
3.2.2 Implicit finite difference approximation of the linear pressure equation	19
3.2.3 IMPES (Implicit pressure explicit saturation) strategy.....	21
4. Newton's method	22
5. Project strategy.....	25
6. Models and results	26
6.1 Reservoir description and fluid properties	26

6.2	Validating models	29
6.2.1	1D Single well model.....	29
6.2.2	1D Two wells model.....	30
6.3	Convergence study	33
6.3.1	Eclipse convergence study	34
6.3.2	tNavigator convergence study.....	37
6.3.3	Comparison of converged models results	39
6.4	Runtimes comparison.....	42
7.	SPE 9 Model	45
8.	Conclusion	50
9.	Bibliography	51

List of Figures

Figure 1.1 General form of MB equation	3
Figure 1.2 Grid illustration	5
Figure 2.1 Grid example	8
Figure 3.1 Finite difference illustration	15
Figure 3.2 Illustration of Pressure propagation in 1D.....	17
Figure 3.3 Illustration of explicit finite difference algorithm	19
Figure 4.1 Illustration of Newton method.....	23
Figure 6.1 1D Single well model	29
Figure 6.2 Single well model reservoir pressure comparison.....	29
Figure 6.3 Single well model oil production rate comparison.....	30
Figure 6.4 Single well model cumulative oil production comparison	30
Figure 6.5 1D Two well model.....	31
Figure 6.6 1D Two well model oil production rate comparison.....	31
Figure 6.7 1D Two well model water production rate comparison	32
Figure 6.8 1D Two well model cumulative oil production comparison	32
Figure 6.9 1D Two well model average reservoir pressure comparison	32
Figure 6.10 Convergence study model	34
Figure 6.11 Oil production rate in Eclipse convergence study runs	35
Figure 6.12 Water production rate in Eclipse convergence study runs	35
Figure 6.13 Cumulative oil produced in Eclipse convergence study runs.....	36
Figure 6.14 Average reservoir pressure in Eclipse convergence study runs	36
Figure 6.15 Oil production rate in tNavigator convergence study runs.....	37
Figure 6.16 Water production rate in tNavigator convergence study runs	38
Figure 6.17 Cumulative oil produced in tNavigator convergence study runs	38
Figure 6.18 Average reservoir pressure in tNavigator convergence study runs	39
Figure 6.19 Oil production rate comparison	40
Figure 6.20 Water production rate comparison	40
Figure 6.21 Cumulative oil produced comparison.....	41
Figure 6.22 Average reservoir pressure comparison	41
Figure 6.23 Runtimes comparison	43
Figure 6.24 Time steps comparison	43
Figure 7.1 Model in 3D view (SPE 9)	45
Figure 7.3 Relative permeability (SPE 9).....	46

Figure 7.4 Capillary pressure (SPE 9)	46
Figure 7.5 Field oil production rate (SPE 9).....	48
Figure 7.6 Average reservoir pressure (SPE 9)	48

List of Tables

Table 6.1 Reservoir Description	26
Table 6.2 PVDO.....	27
Table 6.3 PVTW	27
Table 6.4 Densities.....	27
Table 6.5 Relative permeability values.....	28
Table 6.6 Relative permeability curves	28
Table 6.7 Number of cells per model.....	34
Table 6.8 Grid number of cells per model	42
Table 6.9 Observed runtimes	42
Table 7.1 Time steps (SPE 9)	49

Acknowledgements

I would like to express my sincere gratitude to my supervisor and members of committee for their guidance and the scientific comments during this thesis.

Forever thankful to my family for all the support during this journey, we did it together.

Abstract

This diploma thesis project will focus on the comparison of two black-oil simulation software. The simulators under study are the widely known Eclipse 100 and the relatively new tNavigator ones.

All commercial simulators available in the market are supposed to solve the same differential equation problem using the same approach (finite volumes). However, the performance of them might exhibit significant differences even treating exactly the same simulation problem. Those differences might concern the computing time and/or the obtained results.

In this work we started with simple Cartesian reservoir models and compared their performance against the simulators under study. Since the starting models were of low complexity and the background formulation of both simulators was supposed to be the same the results in terms of run time and simulators predictions should match. By verifying that it was shown that conditions for fair comparison were established and the next comparison step was performed with models of higher complexity. This allowed those fine differences in simulators to impact the prediction outcome, as well as runtime of simulation. As the general comparison strategy of increasing the model complexity is suitable for executing convergence study, this was done along the way. So, became able to evaluate how these two simulators are dealing with error introduced by spatial and temporal discretization as a part of numerical approximation of flow governing equations.

The output data consisting of key parameters (oil/water production rate, average reservoir pressure and cumulative productions) for the respective model were compared along with CPU runtimes.

By finalizing this study, a more solid judgement on performance of these two simulators on the field of black-oil simulations has been built.

1. The Function and Scope of Reservoir simulation

1.1 Introduction

The need for reservoir simulation rises from the necessity of having more accurate ways of predicting reservoir performance under different operating conditions. Since the fact that all petroleum engineering calculations are based on data which carries significant risk regarding accuracy, which is usually magnified by engineering assumptions commonly needed for solving specific problem. This is why, high accuracy risk associated with hydrocarbon recovery project has to be associated and minimized. Factors contributing this risk include complexity of reservoir heterogeneity, anisotropic rock properties, regional variations of fluid properties, complexity of recovery mechanisms and limitations of predictive methods it selves.

The basic function of reservoir simulation is to predict future behavior of reservoir and consequences of various reservoir management scenarios.

1.2 Modeling approaches

Common methods of forecasting reservoir performance generally can be divided into three categories: analogical methods, experimental methods, and mathematical methods. **Analogical** methods use properties of mature reservoirs that are either geographically or petrophysically similar to the target reservoir to attempt to predict reservoir performance of a target reservoir. **Experimental** methods measure physical properties in laboratory models and scale these results to entire reservoir. **Mathematical** methods use equations which are formulating fluid flow in porous media to predict reservoir performance. (Ertekin, 2001)

1.2.1 Analogical methods

In the early stages of field development, such as before drilling phase when there is very limited or no available reservoir data, analogical methods are commonly used in order to predict reservoir performance and perform economic analysis. In this method reservoirs in the same geological basin with similar petrophysical properties are used to predict performance of target reservoir. These methods can be used to estimate recovery factors, production rates, decline

rates, drive mechanisms etc. Reliable results can be achieved when two similar reservoirs are compared and similar development strategies are used. (Ertekin, 2001)

1.2.2 Experimental methods

Experimental methods are playing key role in understanding petroleum reservoirs. Compared to analogical methods they are more often used and mainly in form of corefloods, sandpacks and slim tube tests. Definitely the most commonly used method is coreflood experiment which is generally run on linear cores (reservoir rock sample). The main aim of this experiment is to determine reservoir properties such as porosity and permeability, establishing recovery mechanism and EOR methods testing. (Ertekin, 2001)

1.2.3 Mathematical methods

Mathematical methods are nowadays most commonly used methods. This category includes: material balance method, decline curve analysis, analytical (well test), statistical and reservoir simulation method. Generally majority of these methods can be performed by hand calculation or simple applications of graphical procedures, yet many software packages are available for performing these tasks.

Material balance method or widely called tank model is a mathematical representation of reservoir. Basic principle of this method is mass conservation principle, the mass in the reservoir after production interval (pressure drop D_p) is equal to the mass initially in reservoir minus mass produced during production interval plus the mass added to reservoir (injection of fluid or fluid influx). The simplest way to visualize material balance is that if the measured surface volume of oil, gas and water were returned to a reservoir at the reduced pressure, it must fit exactly into the volume of the total fluid expansion plus the fluid influx. There are many forms of material balance equations which are all derived from a single generalized form (Figure 1.1 General form of MB equation).

The material balance equation and its many different forms have many uses including:

- Confirming the producing mechanism
- Estimating the fluid in place
- Estimating gas cap sizes
- Estimating water influx volumes

- Identifying water influx model parameters
- Estimating producing indices

However material balance method is highly dependent on input data accuracy and meeting the underlying assumptions. The material balance equation does not take in to account spatial variations of rock and fluid properties, thermodynamics of fluid flow in porous media, well positions and is very sensitive to inaccuracies in measured reservoir pressure. Beside of these, significant drawback of this method is necessity of pressure drop, which very often could be prevented by natural water influx or pressure maintenance methods.

$$\begin{aligned}
 & \underbrace{G_{fgi}E_g}_{\text{free-gas expansion}} + \underbrace{N_{foi}E_o}_{\text{free-oil expansion}} + \underbrace{WE_w}_{\text{free-water expansion}} + \underbrace{V_{pi}E_f}_{\text{pore-volume contraction}} + \underbrace{W_e}_{\text{water influx}} \\
 & = \underbrace{(G_p - G_I)\left(\frac{B_g - B_o R_v}{1 - R_v R_s}\right)}_{\text{net gas withdrawal}} + \underbrace{N_p\left(\frac{B_o - B_g R_s}{1 - R_v R_s}\right)}_{\text{oil withdrawal}} + \underbrace{(W_p - W_I)B_w}_{\text{net water withdrawal}}
 \end{aligned}$$

Figure 1.1 General form of MB equation

Where:

- G_{fgi} , N_{foi} , and W are the initial free gas, oil, and water in place, respectively
- G_p , N_p , and W_p are the cumulative produced gas, oil, and water, respectively
- G_I and W_I are the cumulative injected gas and water respectively
- E_g , E_o , E_w , and E_f are the gas, oil, water, and rock (formation) expansivities

Analytical methods are based on exact solution of theoretically derived models. These models usually fully represent physical description of process, but very often results in very complex equations. Which in order to be solved analytically, simplifying assumptions have to be applied. Although these assumptions are applied in order to mathematically solve these equations, physics of the problem is preserved. Analytical methods are commonly used to determine effect of various parameters on reservoir performance.

Statistical methods are using empirical correlations which are statistically derived from historical data of past performances of numerous reservoirs in order to predict future performance of others. Correlations are usually derived from mature reservoirs, and used in nearby new reservoirs. There is wide choice of correlations available in the literature for almost all

1.The Function and Scope of Reservoir simulation

parameters regarding reservoir and fluid properties. Since this method is based on utilization of regression on specific data set. The properties of reservoir under study should be in range of initial regression data set, in order to avoid significant forecasting inaccuracies. Forecasting errors with these techniques are often in range of 20 to 40%.

Reservoir simulation method, the usage of this method as a predictive tool nowadays is standard in petroleum industry. Widespread acceptance of this method can be attributed to significant improvement of computers, mainly regarding processing power and increased memory.

Equations which are describing fluid flow in porous media are highly nonlinear, because of that analytical methods cannot be used and solutions must be obtained with numerical methods. Numerical methods (approximate methods) in contrast to analytical give the values of pressure and saturations only at discrete points in the reservoir. Discretization is the process of converting partial differential equations in algebraic ones. Overall analytical method provides exact solution of specific (simple) problem, where numerical method gives approximation of exact solution for (complex) problem. The discretization process results in system of nonlinear algebraic equations. Which in order to be solved has to be linearized. Once the equations are linearized one of linear equations solving techniques can be used. Generally there are two categories of these methods: direct and iterative methods.

The direct methods are mainly based on Gaussian elimination, and exact solution is obtained after specific number of mathematical operations.

In iterative methods an initial estimate of solution is successively improved until it is reasonably close to the exact solution. The number of mathematical operations is not fixed and it hardly depends on initial estimate, and allowed tolerance (deviation from exact solution).

1.3 Application of Reservoir Simulation

Reservoir simulation is widely used tool for making decisions on the development of new fields, the location of infill wells, and the implementation of enhanced recovery projects. And is generally performed in following steps:

1. Defining objectives of the study. This is done in respect to available data and production history. Defining objectives means setting goals of study, making strategy and defining ranges of expected physically sound outcomes.

1.The Function and Scope of Reservoir simulation

2. Collecting and validating reservoir data. After objective of the study is defined, the next step is reservoir data collecting. It is important that data is validated, and that it satisfies specific needs for building a model. Incorporating additional not necessary data may lead to overload in terms of longer CPU run time or issues with model convergence.
3. Model building. After all necessary data is gathered and validated the simulation model can be built. At this step reservoir is spatially discretized into specific grid configuration (Fig.1.2). And specific reservoir properties are assigned to every grid cell accordingly. This means that every grid cell can have different value of specific property, but reservoir properties are homogeneous inside specific grid cell.
4. History matching. Once the model has been built it has to be tuned, means that specific parameters which by engineering judgment carry the biggest uncertainty have to be manipulated inside the physically sound range in order for the model prediction to match available production history data.
5. Model utilization. Basically at this point reservoir model is ready for any kind of engineering needs, which usually is evaluation of different production schemes and sensitivity analysis of various production and reservoir parameters. (Ertekin, 2001)

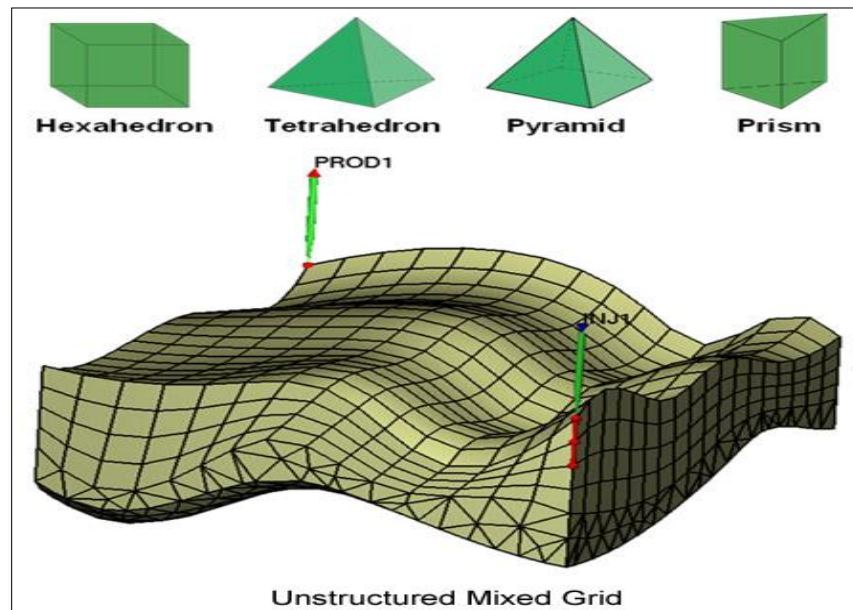


Figure 1.2 Grid illustration

1.4 Reservoir simulators classification

The most common way of classifying reservoir simulators is based on type of reservoir and the fluid simulated, as well as on recovery processes occurring in the subject reservoir. Reservoir simulators can also be classified according to the coordinate system used and the number of phases.

Classification based on reservoir and fluid type generally includes black-oil and compositional reservoir simulators. Black oil simulators are used in situations where recovery processes are insensitive to compositional changes in the reservoir fluid. Compositional simulators are used when recovery processes are sensitive to compositional changes in the reservoir fluid. This usually includes depletion of volatile-oil and gas-condensate reservoirs.

Classifications based on recovery processes include conventional-recovery, chemical-flood, thermal-recovery and miscible-displacement simulators. Basically the natural drive recovery mechanisms (gas cap drive, water drive, solution-gas drive and gravity drainage) can all be modelled with black oil simulator. As well as secondary recovery mechanisms such as water or gas injection, as long as mass transfer effect is negligible. When it comes to more complex depletion mechanisms such as polymer or surfactant floods, there is a need for more advanced simulators such as chemical-flooding simulators or thermal-simulators. These simulators use energy-balance equation in addition to mass-balance equation. (Ertekin, 2001)

2. Model building

This project has been done by utilization of black-oil reservoir simulators. Therefore emphasis was put on black-oil model configuration while other types of reservoir simulators will be briefly mentioned.

Hydrocarbon resources are found within sedimentary rocks that have specific petrophysical characteristics and as such are able to accommodate and transmit fluid. The fluid flow in porous media actually occurs on a micrometer scale in the void space between the rock grains. While the rock zones which carry hydrocarbons are often more than few meters thick and extend several kilometers in the lateral directions. That explains why those rock formations are usually highly heterogeneous in all directions, and what makes a flow in subsurface reservoirs a true multiscale problem. Therefore predicting reservoir performance has a large degree of uncertainty attached, and usually one of main objectives of reservoir simulation is quantification of this uncertainty.

Reservoir simulation is the means by which, one uses a numerical model of the geological and petrophysical characteristics of a hydrocarbon reservoir to analyze and predict fluid behavior in the reservoir over time. In the general form, a reservoir model consists of:

- 1) Geological model in the form of a volumetric grid with cell/face properties that describes the given porous rock formation
- 2) Flow model that describes fluid flow in porous media, usually given as a set of partial differential equations
- 3) Well model that describes the fluid inflow into wellbore, fluid flow within the wellbore and surface facilities.

2.1 Geological model

Description of a reservoir and its petrophysical parameters is usually done through a complex workflow that involves processing data from knowledge of the geologic history of the surrounding basin, seismic and electromagnetic surveys, study of geological analogues (bedrock surface exposures), to rock samples extracted from exploration and production wells. All this data presents input to the reservoir simulation in the form of volumetric grid. Each grid cell provides petrophysical properties that are needed as input to the simulation model, primarily

porosity and permeability. Two petrophysic (Pengbo Lu, 2011) (Dake, 2013) (Reservoir Engineering, 2013) (Ewing, 1983) (Chen, 2001)al properties which are fundamental for all models. The rock porosity (Φ) is a dimensionless quantity that denotes the void volume fraction of the medium available to be occupied by fluids. The permeability (K), is a measure of the rock's ability to transmit a single fluid under certain conditions.

The industry standard is to use so-called stratigraphic grids that are designed to reflect that reservoirs are usually formed through deposition of sediments and consist of stacks of sedimentary beds with different solid particles and varying sizes that extend in the lateral direction. Because of differences in deposition and compaction, the thickness and inclination of each bed will vary in the lateral directions. For the purpose of reservoir simulation, fractures can be considered as cracks or breakage in the rock, across which the layers in the rock have not been displaced. Faults are fractures with displacement.

The most used format, so-called corner-pint grids, consists of a set of hexahedral cells that align so that the cells can be numbered using logical I,J,K index. Each cell has eight logical corner points. One or more corner-points may coincide, and cells that are logical neighbors don't need to have matching faces, which gives rise to unstructured connections. Stratigraphic grids will usually have geometries that deviate far from regular hexahedra, which pose challenges for both discretization methods and nonlinear solvers.

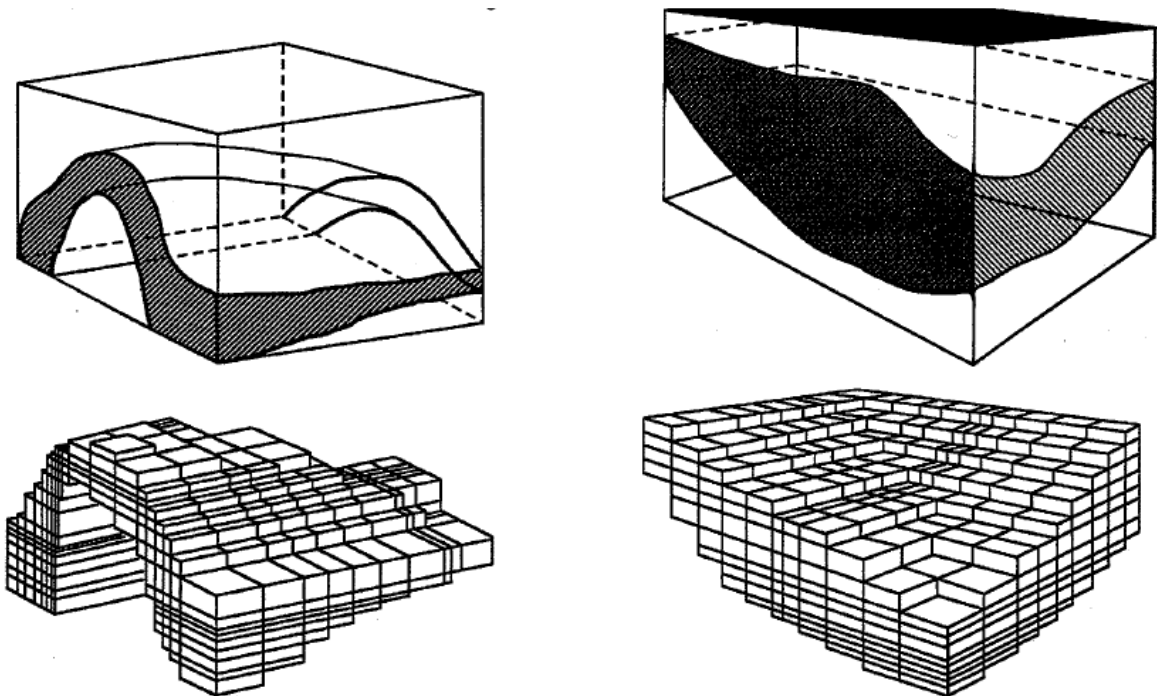


Figure 2.1 Grid example

2.2 Flow models

Second part of reservoir model is mathematical model that describes fluid flow. Respecting the scope of this thesis project we will describe the most common models for isothermal flow.

Single-phase flow. The flow of a single fluid with density ρ through a porous medium is described using the fundamental property of mass conservation.

(2.1)

$$\frac{\partial(\rho\phi)}{\partial t} + \nabla \cdot (\rho\vec{v}) = q.$$

Here, vector v is the velocity and q denote a fluid source/sink term used to model wells. Velocity is related to the fluid pressure p through an empirical relation named after French engineer Henri Darcy:

(2.2)

$$\vec{v} = -\frac{K}{\mu}(\nabla p - \rho\vec{g}),$$

Where K is permeability, μ fluid viscosity and g the gravity vector.

Two-phase flow. The pore space in reservoir is generally occupied by both hydrocarbons and water. Water is often injected in reservoir as part of improved recovery strategy. If the fluids in reservoir are immiscible and separated by a sharp interface, they are referred to as phases. A two-phase system is commonly divided into a wetting and a non-wetting phase, given by the contact angle between the solid surface and the fluid interface on the microscale. On the microscale, the fluids are assumed to be present at the same location, and the volume fraction occupied by each phase is called the saturation of that phase. Therefore, saturation for two-phase system of the wetting and non-wetting phase sums to unity, $S_o+S_w=1$.

During the displacement, the ability of one phase to move is affected by the interaction with the other phase at the pore scale. This effect is represented by the relative permeability Kra ($\alpha = o, n$), which is a dimensionless scaling factor that depends on the saturation and modifies the absolute permeability of wetting (o) and non-wetting (n) phase to account for the rock's reduced ability to transmit each fluid in the presence of the other.

The multiphase extension of Darcy's law:

(2.3)

$$\vec{v}_\alpha = -\frac{Kk_{r\alpha}}{\mu_\alpha}(\nabla p_\alpha - \rho_\alpha \vec{g})$$

This together with the mass conservation of each phase (2.1) forms the basic equation (2.4).

(2.4)

$$\frac{\partial(\rho_\alpha S_\alpha \phi)}{\partial t} + \nabla \cdot (\rho_\alpha \vec{v}_\alpha) = q_\alpha$$

Because of interfacial tension, the pressure in the two phases will differ. This pressure difference is called capillary pressure (2.5) and is usually assumed to be a function of saturation.

(2.5)

$$p_{cnw} = p_n - p_w$$

In order to better reveal the nature of mathematical model, it is common to reformulate (2.3) and (2.4) as a flow equation for fluid pressure and transport equations for saturations. A straightforward manipulation leads to a system for one phase pressure and one saturation in which the capillary pressure appears explicitly. The resulting equations are nonlinear and strongly coupled. To reduce the coupling, one can introduce global pressure (2.6)

(2.6)

$$p = p_n - p_c,$$

where the complementary pressure contains saturation dependant term and is defined as (2.7)

(2.7)

$$\nabla p_c = f_w \nabla p_{cnw}.$$

The dimensionless fractional-flow function (2.8) measures the fraction of the total flow that contains the wetting phase and is defined from the phase mobilities (2.9).

(2.8)

$$f_w = \lambda_w / (\lambda_w + \lambda_n)$$

(2.9)

$$\lambda_\alpha = k_{r\alpha} / \mu_\alpha$$

In the incompressible and immiscible case, (2.3) and (2.4) can now be written as so called fractional form which consists of an elliptic pressure equation (2.10)

(2.10)

$$\nabla \cdot \vec{v} = q, \quad \vec{v} = -K(\lambda_n + \lambda_w) \nabla p + K(\lambda_w \rho_w + \lambda_n \rho_n) \vec{g},$$

for the pressure and the total velocity and a parabolic saturation equation (2.11) for the saturation S_w of the wetting phase.

(2.11)

$$\phi \frac{\partial S_w}{\partial t} + \nabla \cdot f_w(S_w) [\vec{v} + K \lambda_n (\rho_w - \rho_n) \vec{g} + K \lambda_n \nabla p_{cnw}] = \frac{q_w}{\rho_w}$$

The capillary pressure can often be neglected in which case (2.11) becomes hyperbolic.

To solve the system (2.10) and (2.11) numerically, it is common to use sequential solution procedure. First (2.10) is solved to determine the pressure and velocity, which are then held fixed while advancing the saturation at time step dt , and so on.

The black-oil model is the most common used model within reservoir simulation. The model uses a simple PVT description in which the hydrocarbon chemical species are lumped together to form two components at surface conditions, a heavy hydrocarbon component called “oil” and light hydrocarbon component called “gas”, for which the chemical composition remains constant for all times. At reservoir conditions, the gas component may be partially or completely dissolved in the oil phase, forming one or two phases (liquid and vapour) that do not dissolve in the water phase. In more general models hydrocarbons are allowed to be dissolved in water phase, and the water component may be dissolved in two hydrocarbon phases.

The black-oil model is often formulated as conservation of volumes at standard conditions, by introducing formation volume factors (2.12), (V_α and $V_{\alpha s}$ are volumes occupied by a bulk of component α at reservoir and surface conditions). That result in equations (2.13) and (2.14).

(2.12)

$$B_\alpha = V_\alpha / V_{\alpha s}$$

(2.13)

$$\frac{\partial}{\partial t} \left(\frac{\phi \rho_s^\alpha}{B_\alpha} S_\ell \right) + \nabla \cdot \left(\frac{\rho_s^\alpha}{B_\alpha} \vec{v}_\ell \right) = q^\alpha, \quad \alpha = o, w$$

(2.14)

$$\frac{\partial}{\partial t} \left(\frac{\phi \rho_s^g}{B_g} S_g + \frac{\phi R_{so} \rho_s^g}{B_o} S_\ell \right) + \nabla \cdot \left(\frac{\rho_s^g}{B_g} \vec{v}_g + \frac{R_{so} \rho_s^g}{B_o} \vec{v}_\ell \right) = q^g$$

Commercial simulators typically use a fully implicit discretization to solve the nonlinear system (2.13), (2.14). However, there are also several sequential methods that vary in the choice of primary unknowns and the manipulations, linearization, temporal and spatial discretization, and the order in which these operations are applied to derive a set of discrete equations. (Chen, 2001)

2.3 Well models

Simply speaking the well is open hole (conduit) through which fluid can flow in and out of the reservoir. Modern wells are usually cemented and then perforated along specific intervals. Generally there are two types of wells. Production wells, that are designed to extract hydrocarbons and injection wells that are designed for injection of fluid under pressure into reservoir (usually water or gas). The production/injection of fluids is controlled through surface facilities, but wells may also contain advanced down-hole control devices.

The main objective of well models is to accurately represent the inflow from reservoir in the wellbore and provide equations that can be used to compute injection or production rates when the flowing bottom hole pressure is known, or compute the pressure for a given well rate. When the equations presented in previous chapter are discretized using a volumetric grid, the wellbore pressure will be significantly different from the average pressure in the perforated grid block. The diameter of the wellbore is small compared to the size of the block, which implies that large pressure gradients appear in a small region inside the perforated blocks. Modelling injection and production of fluids using point sources gives singularities in the flow field and is seldom used in practice. Instead, one uses an analytical or semi-analytical solution of the form (2.15) to relate the wellbore pressure P_{wb} to the numerically computed pressure P_b inside the perforated blocks.

(2.15)

$$-q = WI(p_b - p_{wb})$$

Here, the well index WI accounts for the geometric characteristics of the well and the properties of the surrounding rock.

The first and still the most used model was developed by Peaceman (2.16). Assuming steady state radial flow and a 7-point finite difference discretization, the well index for an isotropic medium with permeability K represented on Cartesian grid represented by (2.16).

(2.16)

$$WI = \frac{2\pi K \Delta z}{\ln(r_0/r_w)},$$

(2.17)

$$r_0 = 0.14(\Delta x^2 + \Delta y^2)^{\frac{1}{2}}$$

Here, r_w is the radius of the well and r_0 is the effective block radius at which the steady-state flowing pressure equals the numerically computed block pressure. The Peaceman model has later been extended to multiphase flows, anisotropic media, horizontal wells, non-square grids, and other discretization schemes, as well as to incorporate gravity effects, changes in near-well permeability (skin), and non-Darcy effect. More advanced models describe the flow inside the wellbore and how this flow is coupled with surface controls and processing facilities.

3. Numerical methods in reservoir simulation

The multi-phase flow equations for real systems are so complex that it is not possible to solve them analytically. In practice these equations can only be solved numerically. The most commonly applied numerical methods are based on finite difference approximations of the flow equations. In this chapter we will briefly review these methods.

3.1 Review of finite difference

The main task of finite difference method is to approximate derivatives of a function. In order to simply present this method we will utilize graphical illustration (Figure 3.1) on a way to approximate derivative of function $P(x)$.

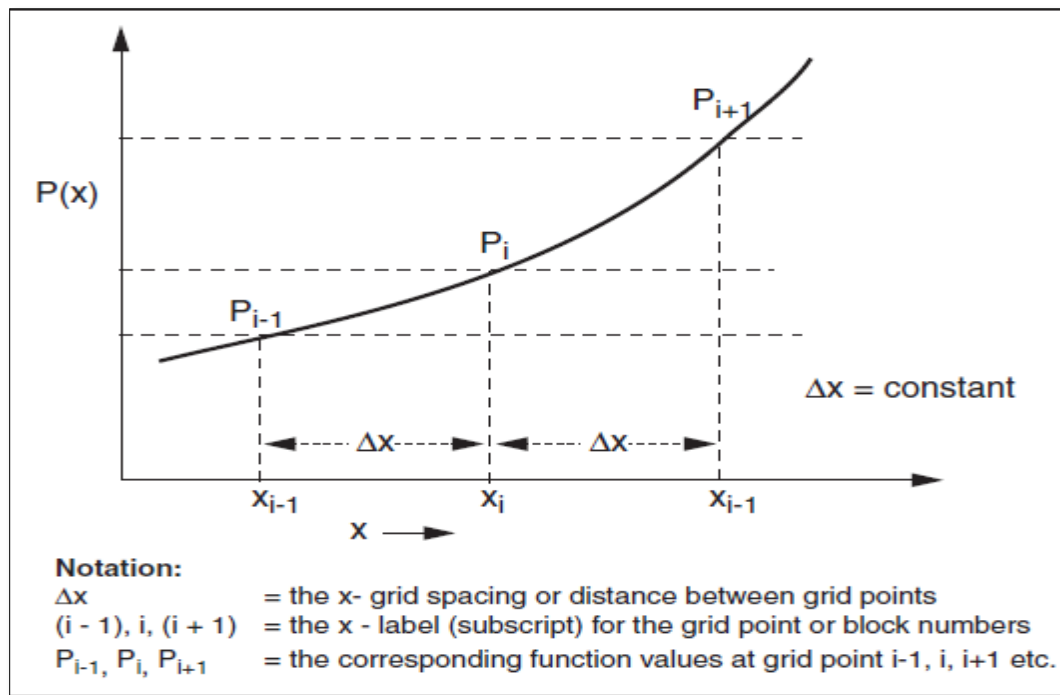


Figure 3.1 Finite difference illustration

Forward difference: we approximate the slope between P_i and P_{i+1} as being $\left(\frac{dP}{dx}\right)_i$ at x_i to obtain:

(3.1)

$$\left(\frac{dP}{dx}\right)_{ifd} = \frac{P_{i+1} - P_i}{\Delta x}$$

Backward difference: we approximate the slope between P_{i-1} and P_i as being $\left(\frac{dP}{dx}\right)_i$ at x_i to obtain:

(3.2)

$$\left(\frac{dP}{dx}\right)_{ibd} = \frac{P_i - P_{i-1}}{\Delta x}$$

Central difference: we take the average of forward and backward difference approximation to give us $\left(\frac{dP}{dx}\right)_i$ at x_i :

(3.3)

$$\begin{aligned} \left(\frac{dP}{dx}\right)_{icd} &= \frac{1}{2} \left[\left(\frac{dP}{dx}\right)_{ifd} + \left(\frac{dP}{dx}\right)_{ibd} \right] = \frac{1}{2} \left[\frac{P_{i+1} - P_i}{\Delta x} + \frac{P_i - P_{i-1}}{\Delta x} \right] \\ \left(\frac{dP}{dx}\right)_{icd} &= \left[\frac{P_{i+1} - P_{i-1}}{2 \cdot \Delta x} \right] \end{aligned}$$

3.2 Application of finite difference on flow equation

Due to the overall complexity of problem, in this chapter we will focus on explaining general principle of PDE's discretization on linear pressure equation in its simplest form, but satisfactory for demonstration purpose.

3.2.1 Explicit finite difference approximation of the linear pressure equation

The flow equations are actually partial differential equations (PDE's), with the unknowns, $P(x,t)$ and $S(x,t)$, dependent on both space and time. As previously said, for this purpose we will utilize simplified pressure equations (3.1), which is linear and has known analytical solutions for various boundary conditions. However, this will be neglected and we will apply numerical methods as an example of how to use finite differences to solve PDE's numerically. As even further simplification of this problem, we will assume term of hydraulic diffusivity $\left(\frac{k}{c\mu\Phi}\right)$ constant. This will result with equation (3.2).

(3.1)

$$\left(\frac{\partial P}{\partial t}\right) = \frac{k}{c\phi\mu} \left(\frac{\partial^2 P}{\partial x^2}\right)$$

(3.2)

$$\left(\frac{\partial P}{\partial t}\right) = \left(\frac{\partial^2 P}{\partial x^2}\right)$$

This is the pressure equation for a 1D system where $0 \leq x \leq L$ where L is length of the system. We can visualize this physically using Figure 3.2. After the system is held constant at $P = P_0$, the inlet pressure is raised (at $x=0$) instantly to $P = P_{in}$ while the outlet pressure is held at $P_{out}=P_0$.

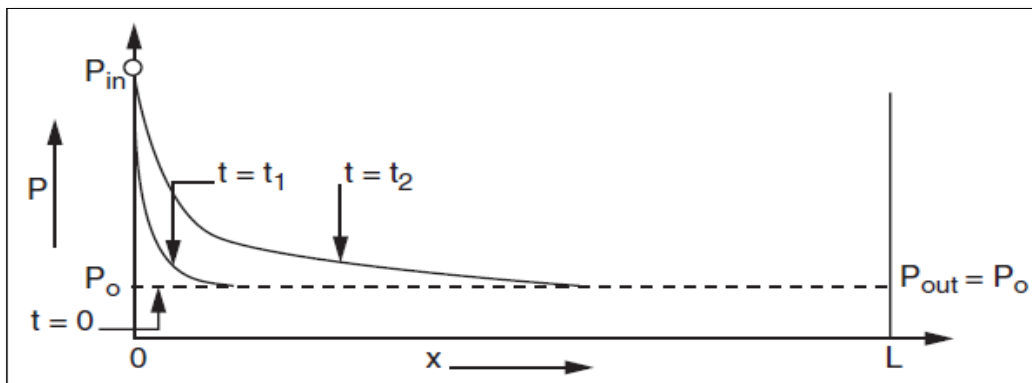


Figure 3.2 Illustration of Pressure propagation in 1D

These pressures, P_{in} and P_{out} represent the constant pressure boundary conditions. This problem is approached using finite difference as follows:

- discretize the x-direction by dividing into numerical grid of size Δx ;
- choose a time step, Δt ;
- use the following notation

n, time level

i, grid block label

P_i^n , current (known) P at time level

P_i^{n+1} , new (unknown) P at time level

- fix the boundary conditions

$P_1 = P_{in}$ and $P_{out} = P_0$ which are fixed for all t.

- Apply finite difference for equation (3.2) using the above notation to obtain:

(3.3)

$$\left(\frac{\partial P}{\partial t} \right)_i \approx \frac{P_i^{n+1} - P_i^n}{\Delta t}$$

and

(3.4)

$$\left(\frac{\partial^2 P}{\partial x^2} \right)_i \approx \frac{P_{i+1}^n + P_{i-1}^n - 2P_i^n}{\Delta x^2}$$

Equating the numerical finite difference approximations of each of the above derivatives as required by the original PDE, equation (3.2) gives:

(3.5)

$$\frac{P_i^{n+1} - P_i^n}{\Delta t} \approx \frac{P_{i+1}^n + P_{i-1}^n - 2P_i^n}{\Delta x^2}$$

which by some simple manipulation can be expressed explicitly for P_i^{n+1} , the only unknown in the above equation:

(3.6)

$$P_i^{n+1} = P_i^n + \frac{\Delta t}{\Delta x^2} (P_{i+1}^n + P_{i-1}^n - 2P_i^n)$$

Equation (3.6) provides algorithm for propagating solution of PDE equation (3.2), forward in time from the given set of initial conditions.

The assumption that we made in order to obtain equation (3.4) was that the spatial derivative was taken at the n (known) time level. This allowed us to develop explicit formula for P_i^{n+1} . This method is therefore known as explicit finite difference method.

Another way to represent this explicit finite difference solution to PDE is shown in Figure 3.3.

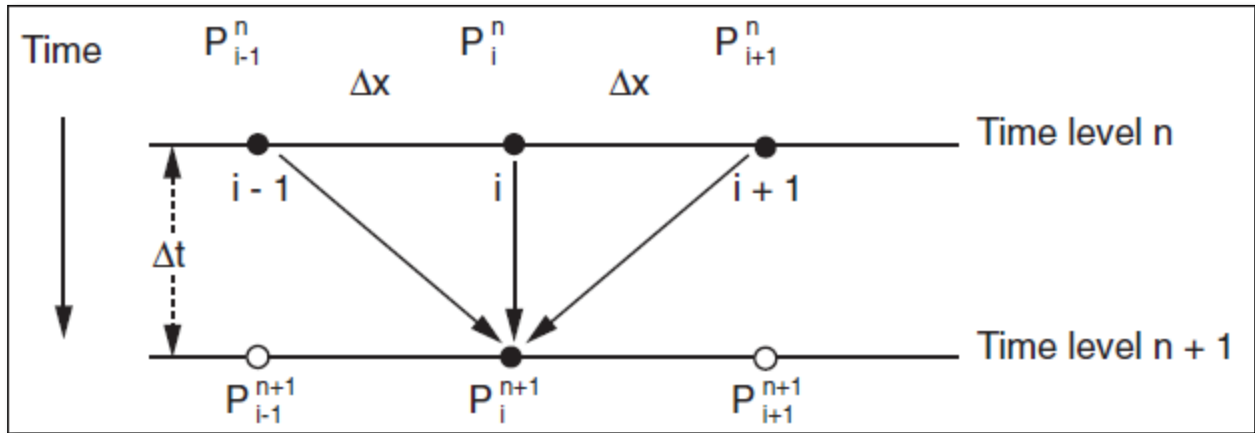


Figure 3.3 Illustration of explicit finite difference algorithm

Cons of this method:

- Sensitivity to Δt , if Δt is too big numerical solution of PDE gives physically impossible results (negative pressure can occur). In fact solution is unstable for larger time steps.
- Sensitivity to Δx , the effect of grid refinement is that, as the grid blocks get smaller the answer should get more accurate. Although to make this happen time step should be reduced as well.

3.2.2 Implicit finite difference approximation of the linear pressure equation

If we repeat the procedure of explicit finite difference up to a point of deriving equation (3.4), and instead of taking pressure values from n (known) step we take it from $n+1$ step. It will result with spatial derivative equation (3.7).

(3.7)

$$\left(\frac{\partial^2 P}{\partial x^2}\right)_i \approx \frac{P_{i+1}^{n+1} + P_{i-1}^{n+1} - 2P_i^{n+1}}{\Delta x^2}$$

While the time derivative stays the same as (3.3).

As previously we can now equate (3.3) and (3.7) equation to obtain:

(3.8)

$$\frac{P_i^{n+1} - P_i^n}{\Delta t} \approx \frac{P_{i+1}^{n+1} + P_{i-1}^{n+1} - 2P_i^{n+1}}{\Delta x^2}$$

If we try and manipulate equation (3.8) in similar way as (3.5), we will easily realize that this won't be possible, because it appears that now we have three unknowns P_{i-1}^{n+1} , P_i^{n+1} and P_{i+1}^{n+1} . Therefore, in order to solve this we have to rearrange equation (3.8) in following fashion:

(3.9)

$$P_{i-1}^{n+1} - \left(2 + \frac{\Delta x^2}{\Delta t}\right)P_i^{n+1} + P_{i+1}^{n+1} = -\left(\frac{\Delta x^2}{\Delta t}\right)P_i^n$$

Where all the unknowns are on the left-hand side and term on right hand side is known, since it is from the n (known) time level. This expression gives us possibility to rewrite this equation as follows:

(3.10)

$$a_{i-1}P_{i-1}^{n+1} + a_iP_i^{n+1} + a_{i+1}P_{i+1}^{n+1} = b_i$$

Where:

$$a_{i-1} = 1,$$

$$a_i = \left(2 + \frac{\Delta x^2}{\Delta t}\right),$$

$$a_{i+1} = 1 \text{ and } b_i = -\left(\frac{\Delta x^2}{\Delta t}\right)P_i^n \text{ are all constants.}$$

The a_i do not change throughout the calculation but the quantity b_i is updated at each time step as newly calculated P^{n+1} is set as P_n . Solving this problem will always result in a system of equation which for example of 20 grid points will give 18 equations, which combined with boundary conditions can be solved. And it generally yields a sparse, tridiagonal matrix.

3.2.3 IMPES (Implicit pressure explicit saturation) strategy

The idea behind IMPES formulation lies somewhere between implicit and explicit formulation, after we discretize the flow equations explicitly, we take constituents from next time step. In the IMPES method we use time-lagged values of the saturation (from the known/previous step), the pressure equation is linearized and can be solved implicitly for the pressure. After the latest pressure value is obtained, we can solve for saturation explicitly, and repeat the process. That makes IMPES an iterative process, which needs to be repeated until it converges. However, IMPES has limitations in terms of time step size. If Δt is too large, IMPES method may become unstable and give unphysical results.

4. Newton's method

The journey of runtime performance enhancement of numerical reservoir simulators never ended since reservoir simulator was invented in early 1950's. Obviously motivated by business needs for large simulation models and needs for more detailed and less uncertain reservoir management, there have been numerous research and development efforts focusing on different aspects of numerical reservoir simulators seeking speed improvement. The major research areas include massive parallel computing, fast and more efficient flash calculations and advanced linear solver techniques targeting reservoir simulation. Coincidentally, total simulation runtime is directly related to number of simulation cells, degree of model complexity and number of simulations runs.

In this paragraph we will briefly present one of the most commonly used techniques for solving sets of nonlinear equations in reservoir simulators.

In the static reservoir simulation model, the subsurface geological setting is mapped and discretized accordingly into grid cells. Every cell is assigned specific petrophysical property. Within the dynamic reservoir simulation, flow is established and modeled with fluid flow equations previously presented. This means that each grid cell has assigned equation set that describes the flow into the cell, the flow out of the cell and the accumulation within the block. The solution of the equations within the cell varies over time. In a numerical reservoir simulator, solutions are discretized both in space (simulation grid) and in time (discrete time steps), resulting in a fully coupled nonlinear discrete system. The most widely-used nonlinear solver technique is the Newton's method, an iterative root-finding method, for solving reservoir simulation equations at each time step. In this method, the set of simulation equations are cast into a form that makes the solution an exercise in finding the zeros of a function, finding x such that $f(x) = 0$.

Figure 4.1 illustrates the Newton's method for a single-variable function. The red curve is the function $f(x)$ and we seek to find the value x where $f(x) = 0$, the red point. The initial guess is x_0 . The second guess is calculated by taking the tangent to $f(x)$ at x_0 , the blue line and applying the formula $x_1 = x_0 - \frac{f(x_0)}{f'(x_0)}$. This formula is the classic Newton-Raphson method. Here $f'(x)$ denotes the derivative of the function $f(x)$ and is the slope of the tangent line. The third guess x_2 , uses the tangent at the second guess (x_1), the green line, and applies the same formula $x_2 = x_1 - \frac{f(x_1)}{f'(x_1)}$. Continuing this iterative algorithm, we can get very close to the root of $f(x)$ in a modest number of iterations.

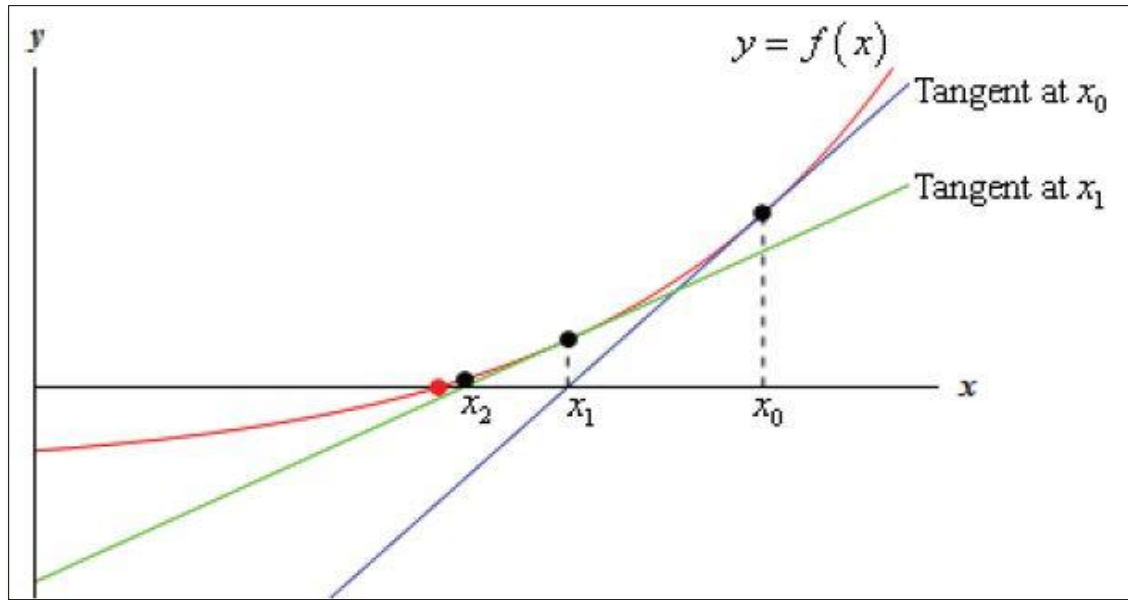


Figure 4.1 Illustration of Newton method

Numerical reservoir simulators have taken this idea and expanded it to solve for the many thousands of equations at each time step. Instead of solving one equation with unknown, we are solving a set of equations corresponding to a set of unknowns $\{x_1, x_2, \dots, x_n\}$.

$$\begin{aligned}
 f_1(x_1, \dots, x_n) &= 0 \\
 f_2(x_1, \dots, x_n) &= 0 \\
 &\vdots \\
 f_n(x_1, \dots, x_n) &= 0
 \end{aligned}$$

The unknowns in the equation set are typically pressures and saturations at each simulation cell. To apply Newton's method to this system of equations, we need to calculate tangent of the function, in the same fashion as described above for the single-variable equation. The tangent of the multi-variant function is called the Jacobian matrix, J , composed of the derivatives of the functions with respect to the unknowns.

$$J = \begin{bmatrix} \frac{\partial f_1}{\partial x_1} & \dots & \frac{\partial f_1}{\partial x_n} \\ \vdots & \ddots & \vdots \\ \frac{\partial f_n}{\partial x_1} & \dots & \frac{\partial f_n}{\partial x_n} \end{bmatrix}$$

As in the case with the single variable equation, we start with an initial guess \vec{x}_0 , where \vec{x}_0 is a vector of solutions and each subsequent guess is formed in the same manner as that for a single variable.

$$\vec{x}^{k+1} = \vec{x}^k - (f(\vec{x}^k)/J(\vec{x}^k))$$

This equation can be rewritten as

$$J(\vec{x}^k) \delta \vec{x}^{k+1} = -f(\vec{x}^k)$$

$$\vec{x}^{k+1} = \vec{x}^k + \delta \vec{x}^k$$

The solution is considered to be converged when the norm of either the solution change $\delta \vec{x}^{k+1} = (\vec{x}^{k+1} - \vec{x}^k)$ or the residual $f(\vec{x}^k)$ drops below the present convergence threshold ϵ .

In general, the fully implicit scheme solved, with the Newton's method commands substantial CPU time and large memory footprint. There have been many attempts to reduce the CPU overhead associated with the fully implicit scheme, without sacrificing the benefits from fully implicit method unconditional stability.

5. Project strategy

Usage of same personal computer for all comparative runs was a fundamental condition. Main PC information are listed below:

Processor: Intel® Core™i7-7700HQ CPU @ 2.8GHz

RAM memory:16 GB

System: 64-bit Operating System, x64-based processor.

Primary goal was to ensure fair comparison environment, which was fulfilled by creating simple Cartesian models (oil-water, low number of grid cells, uniform porosity and permeability reservoir and single production well operating) in which depletion was driven by natural drive mechanisms. Aim of this simulation runs was to obtain same output results due to low complexity of model which is not allowing to any possible fine differences in simulator to take place. Based on the fact that overall configuration of simulators is developed on same principles with possibly only minor differences. If matching of output results from both simulators is obtained, that was taken as a sign of fair comparison environment.

After ensuring that primary goal is achieved, the further strategy was to continue increasing complexity of model. That was executed mainly by increasing number of grid blocks, and introducing models with more complex recovery mechanisms such as waterflooding. During whole study due to simplification and consistency reasons reservoir description including geometry, petrophysical properties and fluid properties will remain same in all models beside of SPE 9 Model. By increasing complexity of models, we expected those possible fine differences in simulators to take place and express in a way of different simulation output. Emphasis was on oil production rates, water production rate, average reservoir pressure and cumulative production. As well at this point, we expected to observe noticeable CPU run time differences due to higher complexity of models, which allowed efficiency of simulator solvers to affect run time of simulations. According to this, briefly said we were increasing complexity of models, while monitoring the simulation output and CPU run time of simulators. Following this work, we performed brief model convergence (minimization of numerical error) study in both simulators since the strategy of increasing model complexity by increasing number of cells is suitable for this study.

While running the simulations we were continuously monitoring the previously mentioned parameters, in order to ensure that all results were physically sound or in range of expected values if fictive values of any of parameters were used in model itself, and that there are no severe differences which may be caused by input model errors.

After results were generated, the comparison plots of chosen output parameters were built for every specific model in order to visualize eventual differences and CPU run times were compared. Based on this we concluded with evaluation of chosen reservoir simulators.

6. Models and results

6.1 Reservoir description and fluid properties

In this chapter we will present reservoir description and fluid properties which will remain constant through all models used in this study.

Geometrical and petrophysical description is provided in Table 6.1. As it can be seen reservoir is dominantly extending in horizontal (X) direction with significantly thinner width (Y) and vertical extent (Z). Permeability distribution is homogeneous in given directions. PVT properties of oil are presented in Table 6.2, please note that gas density is provided in order to meet minimum required data for input model despite of the fact that gas phase is not defined as existing phase. Oil could be characterized as light to medium heavy oil (Table 6.4). In order to acquire relative permeability values Corey correlation model was built in CMG Simulation Builder (Table 6.5).

Reservoir description	
Direction	Dimension [ft]
X	4500
Y	150
Z	150
Depth [ft]	8000
Petrophysical properties	
Porosity %	20
Direction	Permeability [md]
X	200
Y	150
Z	50

Table 6.1 Reservoir Description

Pressure [psi]	B _o	μ [cP]
2034	1.339	0.668869
2258	1.335	0.7
2515	1.33	0.75
2765	1.326	0.81
3015	1.322	0.86
3265	1.318	0.91
3515	1.314	1
3765	1.31	1.19
4015	1.307	1.197
4515	1.3	1.25
5015	1.294	1.3

Table 6.2 PVDO

PVTW			
Pressure [psi]	B _w	Compressibility [1/psi]	μ [cP]
4500	1.02	3.00E-06	0.8

Table 6.3 PVTW

Density [lbs/cft]	
Oil	49
Water	63
Gas	0.01

Table 6.4 Densities

Sw	Krw	Krow
0.200	0.000	0.700
0.225	0.000	0.632
0.250	0.000	0.567
0.278	0.003	0.498
0.306	0.013	0.434
0.334	0.028	0.374
0.363	0.051	0.319
0.419	0.114	0.221
0.447	0.155	0.179
0.475	0.203	0.142
0.503	0.256	0.109
0.531	0.316	0.080
0.559	0.383	0.055
0.588	0.456	0.035
0.616	0.535	0.020
0.644	0.620	0.009
0.672	0.712	0.002
0.700	0.810	0.000
0.725	0.903	0.000
0.750	1.000	0.000

Table 6.5 Relative permeability values

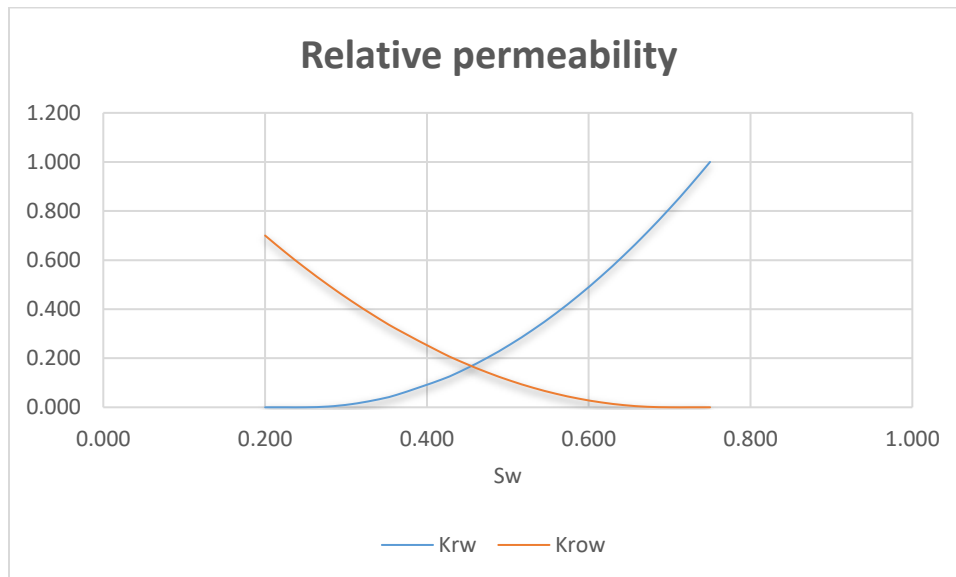


Table 6.6 Relative permeability curves

6.2 Validating models

In this study we started with a simple 1D Cartesian model, in order to establish fair comparison results by matching simulation output results. For this purpose we utilized two models with equal number of grid cells (10) and same reservoir description (Table 6.1 Reservoir Description). The difference in these two models is the depletion mechanism. In which, Model 1 has a single production well and the depletion is driven by natural drive mechanisms, while Model 2 has one production well and one injection well and as so the depletion is water driven.

6.2.1 1D Single well model

Number of grid cells 10x1x1. Well location 1, 1, 1 (Figure 6.2). Initial reservoir pressure 4500 psi. Well will be operating with constant bottomhole pressure (BHP) of 2000 psi.

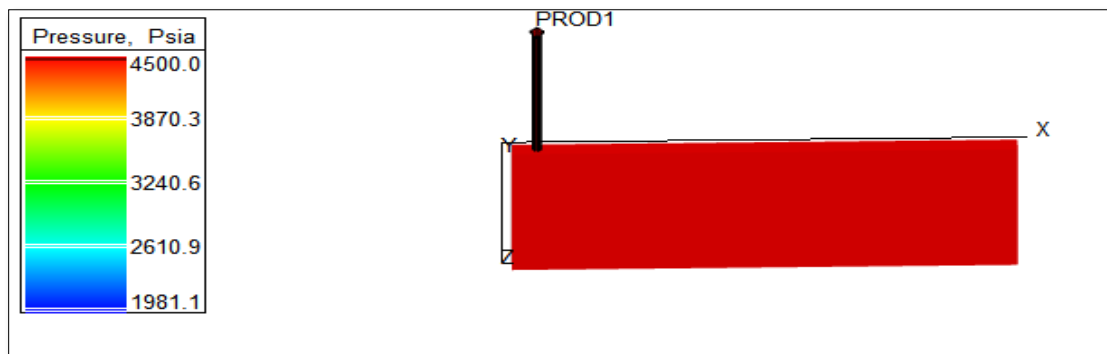


Figure 6.1 1D Single well model

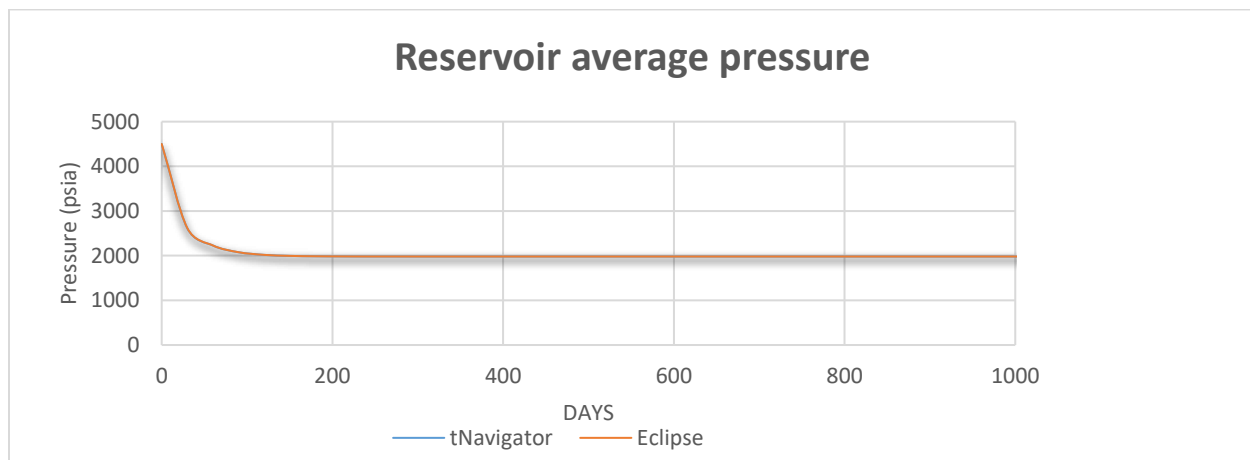


Figure 6.2 Single well model reservoir pressure comparison

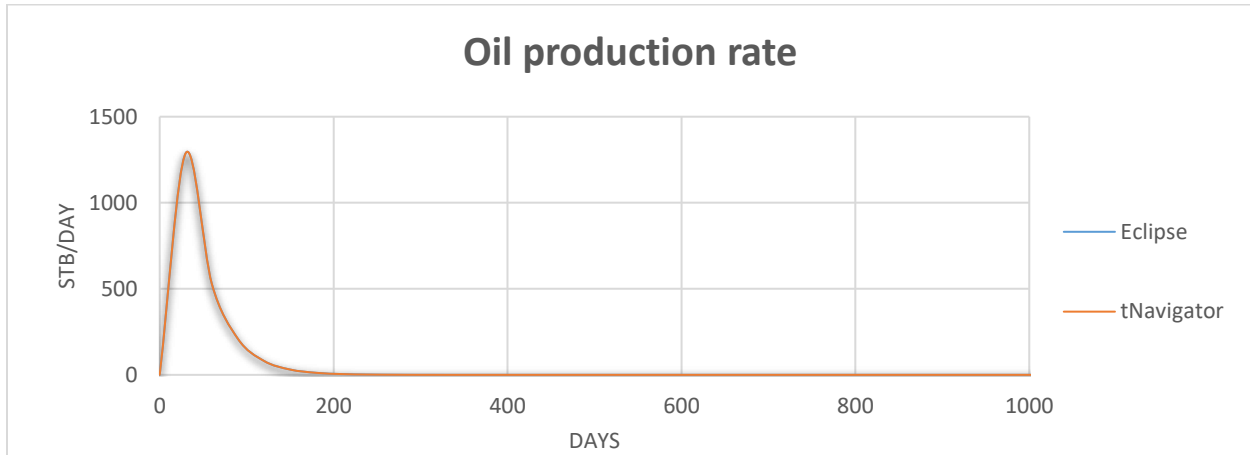


Figure 6.3 Single well model oil production rate comparison

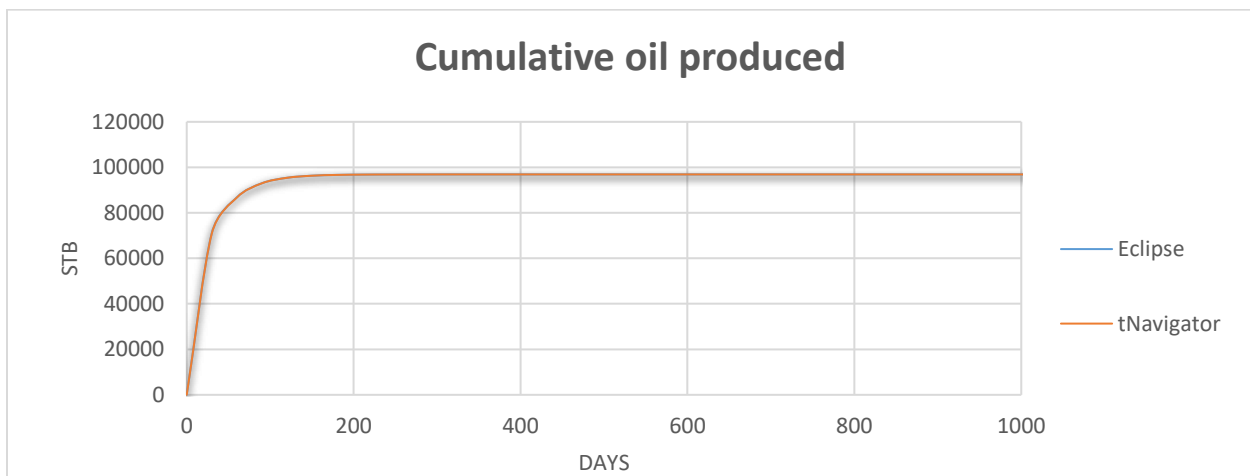


Figure 6.4 Single well model cumulative oil production comparison

As it can be seen from the obtained results, the peak of production rate was reached quickly and it was followed with a rapid decay of production rate and finally the end of production. This can be easily explained by the fact that depletion is done by limited natural drive (compaction drive). The results from both of the simulators are perfectly matching.

6.2.2 1D Two wells model

Number of grid cells 10x1x1. Production well location (1, 1, 1), injection well location (10, 1, 1). (Figure 6.5). Initial reservoir pressure 4500 psi. Production well was operating with constant

bottomhole pressure (BHP) of 2000 psi, injection well was operating with constant injection rate of 2000bbl/day. Both of the wells are operating from the start of simulation.

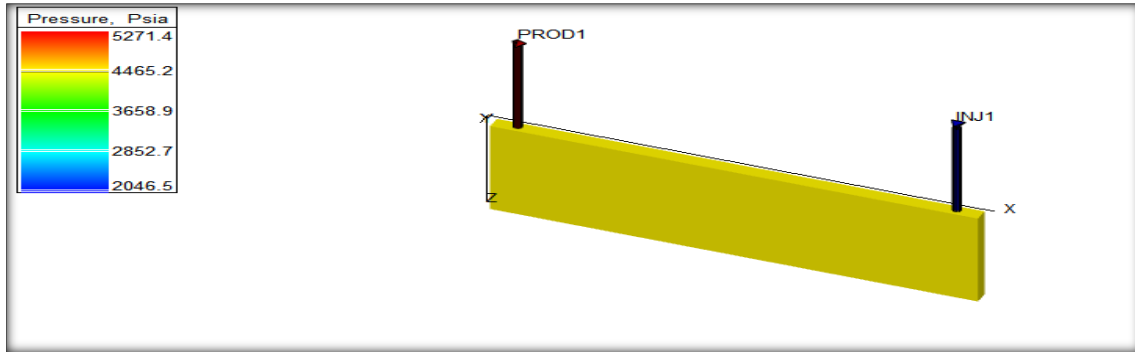


Figure 6.5 1D Two well model

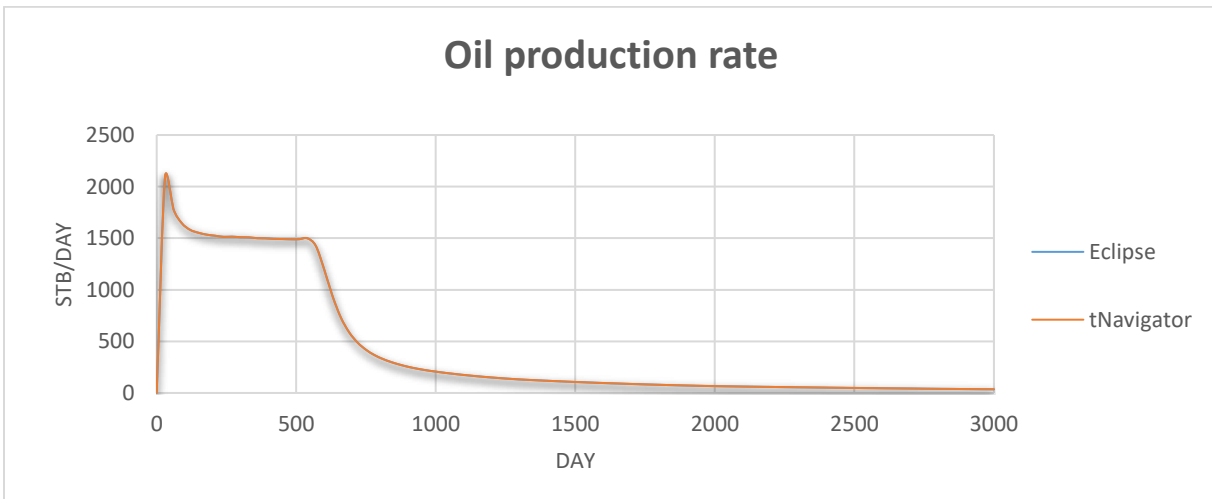


Figure 6.6 1D Two well model oil production rate comparison

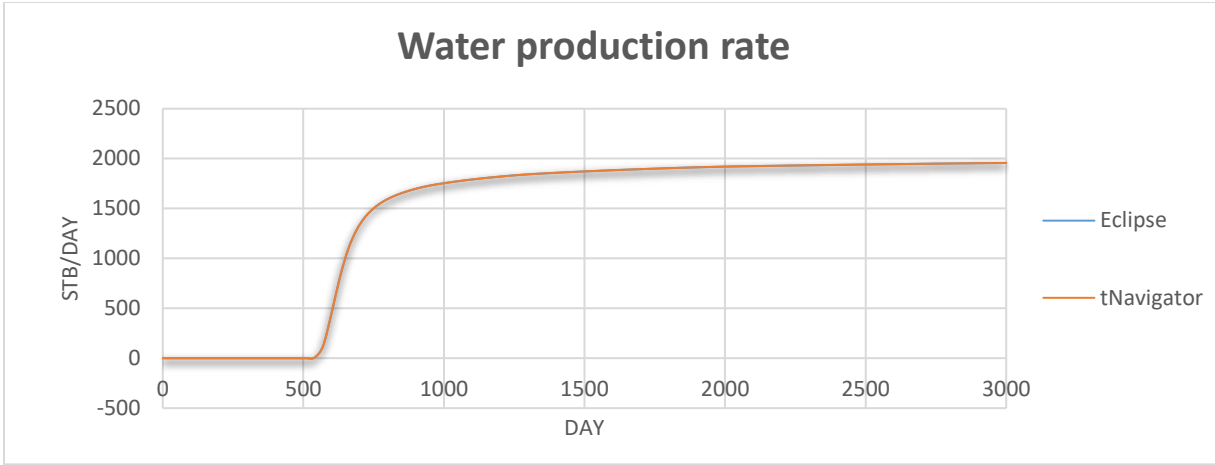


Figure 6.7 1D Two well model water production rate comparison

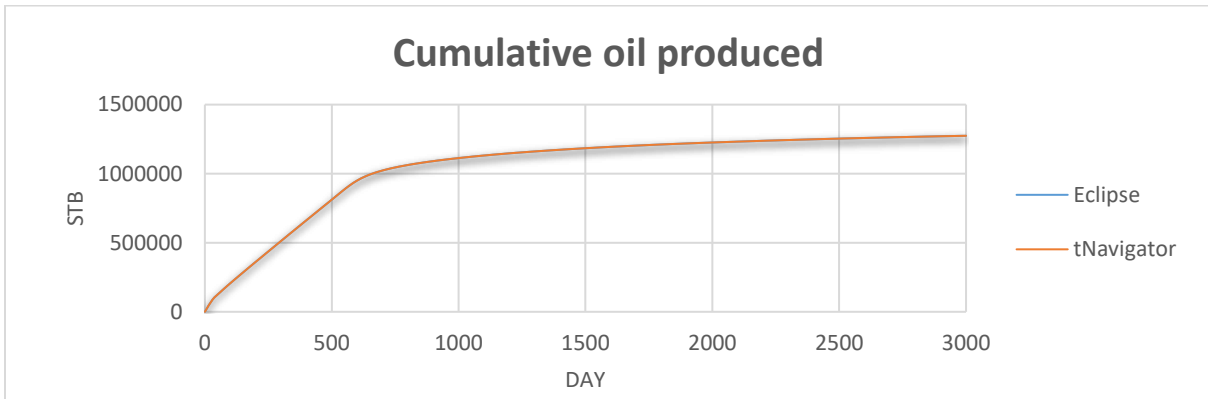


Figure 6.8 1D Two well model cumulative oil production comparison

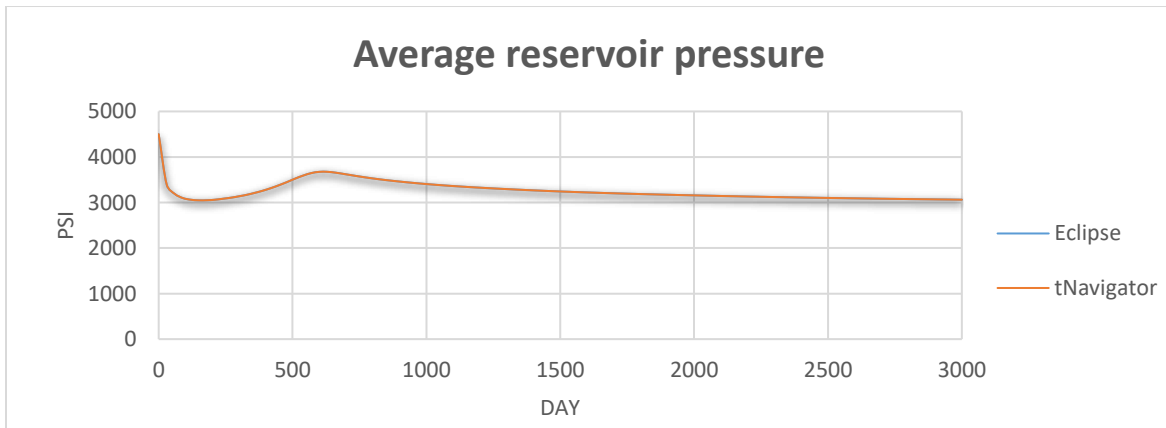


Figure 6.9 1D Two well model average reservoir pressure comparison

As we can see from obtained results, we have peak of production rate quickly after the start of production which is caused by natural drive mechanism and that is followed with rapid decay of production rate until the waterflooding regime takes place. After that we can observe formation of production plateau. Production plateau extends to the moment of water breakthrough, which causes production well water cut to start growing., and further decay of oil production rate until the moment when only flowing phase is water. All of that is as well depicted on average reservoir pressure. We can see that perfect match of output results is achieved in both simulators that we will take as a final evaluation of fairness in this comparison study and as approval to continue with more complex models.

6.3 Convergence study

In this phase we were dealing with numerical dispersion introduced by spatial discretization, and observed how these two simulators deal with similar problem. In this phase we started monitoring CPU runtime of simulations, since complexity of models was gradually increasing as a part of convergence study procedure. This procedure includes a multiple simulation runs, where only variable will be number of grid cells. General principle is to start from low number of grid cells and keep gradually increasing this variable, while the output results of simulation will be approaching exact solution by every next update. During this study the only constrain was runtime of simulation, which should stay in tolerable range (often decided by user). Practically it is a balance between acceptable numerical error and satisfactory runtime duration. This study provided as with suitable environment for CPU runtime comparison, because as previously explained we had gradual growth of grid cells and model complexity.

Model was built with previously presented reservoir and fluid properties (Chapter 6.1), with a difference in reservoir dimensions (4500x4500x300 [ft]), OWC depth of 8350 [ft] and waterflooding depletion mechanism. Including the 4 production wells which were always located in the grid corners and 1 injection well located in the center of grid. Production wells were producing with constant bottomhole pressure (2000 psi), while injection well was rate controlled (50000 bbl/day). Injection rate has been given fictive value in order to keep average reservoir pressure higher than production wells BHPs for whole period of simulation and avoid shutdown of production wells.

Chosen grid dimensions will be presented in Table 6.7.

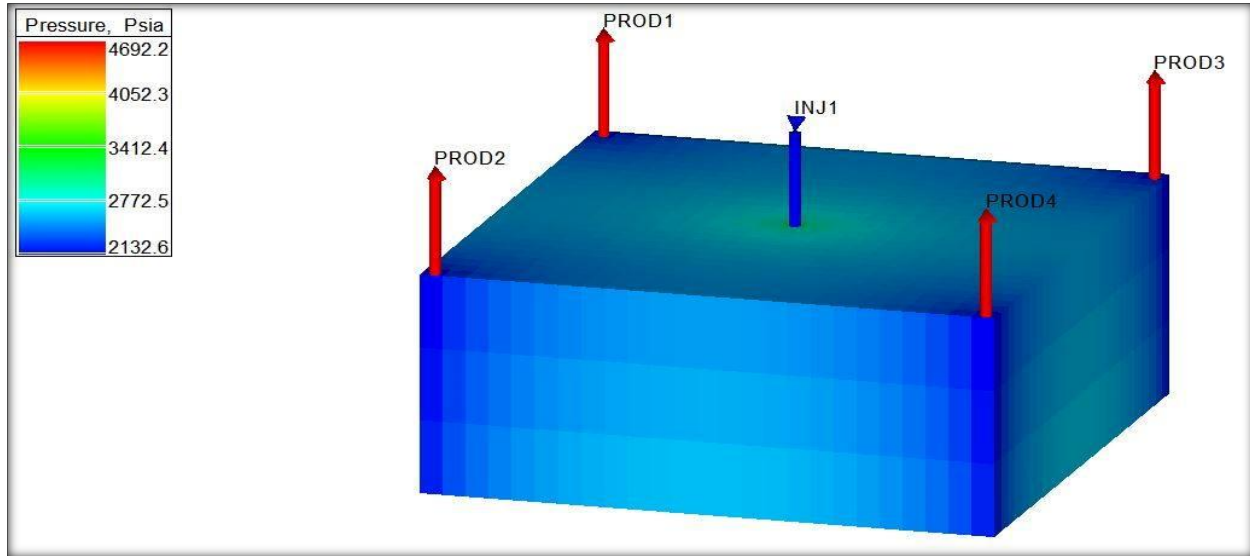


Figure 6.10 Convergence study model

Model	I	II	III	IV
X-direction number of cells	11	25	75	125
Y-direction number of cells	11	25	75	125
Z-direction number of cells	3	3	3	3
Total number of cells	363	1875	16875	46875

Table 6.7 Number of cells per model

Firstly, we performed a study independently on both simulators and decided which model satisfies constraints, regarding acceptable numerical error and least runtime. After selecting appropriate model in case of both simulators, their output results were compared.

6.3.1 Eclipse convergence study

As previously explained, gradually increased numbers of cells, until no further improvement in results were obtained. Since theoretically we could have continued increasing number of grid cells infinitely and by every step, we would be closer to real solution. That would be followed by simulation runtime going towards infinity. Since in reality we cannot afford that, simulation runtime is one of constraints in this study.

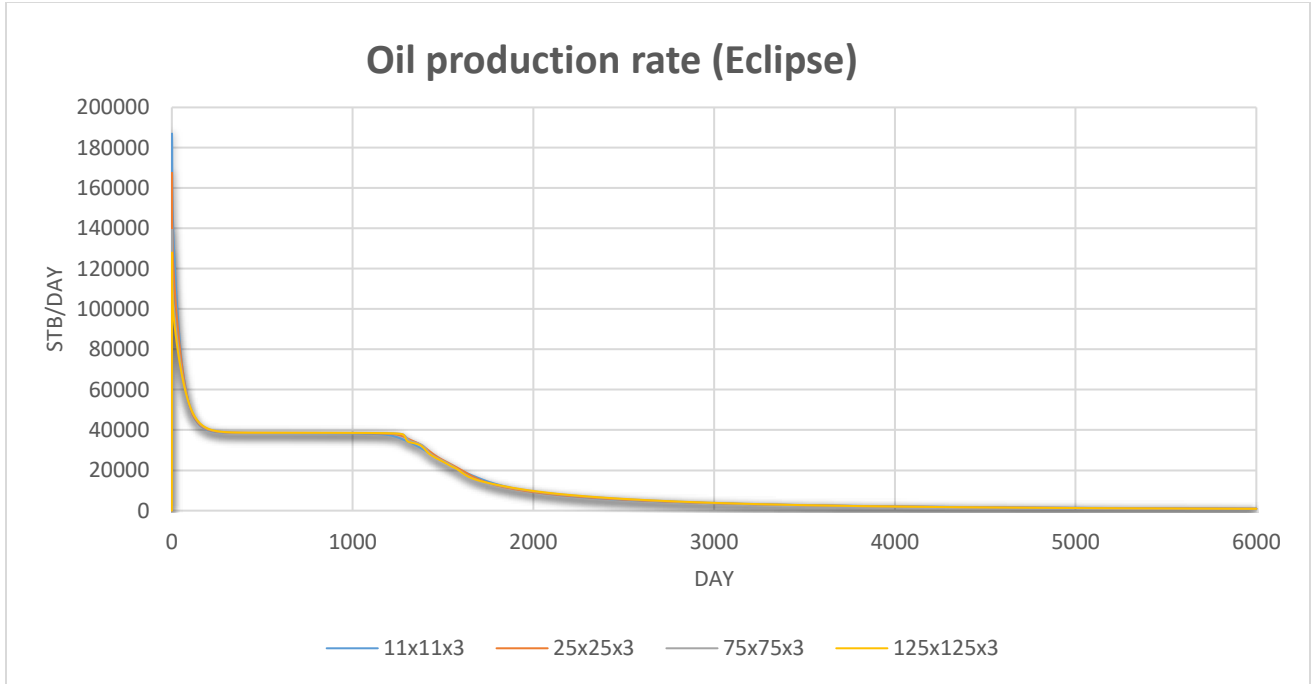


Figure 6.11 Oil production rate in Eclipse convergence study runs

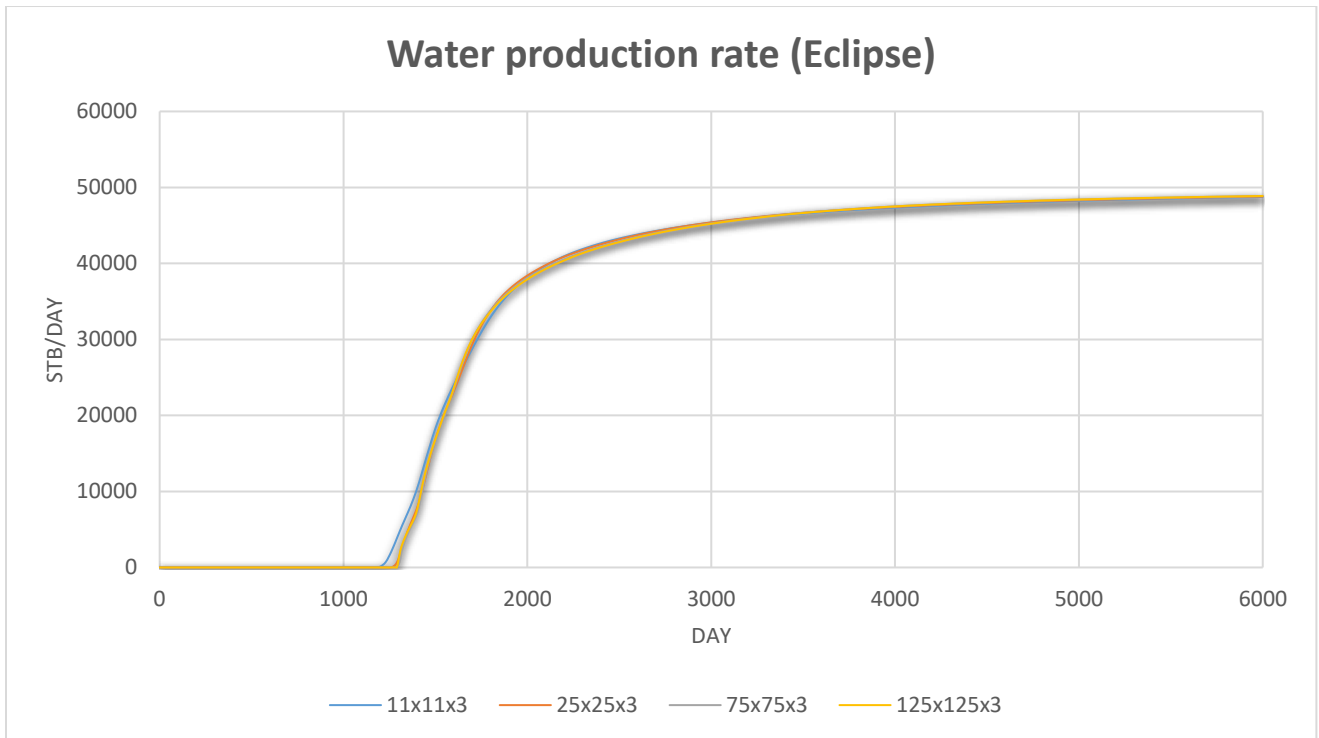


Figure 6.12 Water production rate in Eclipse convergence study runs

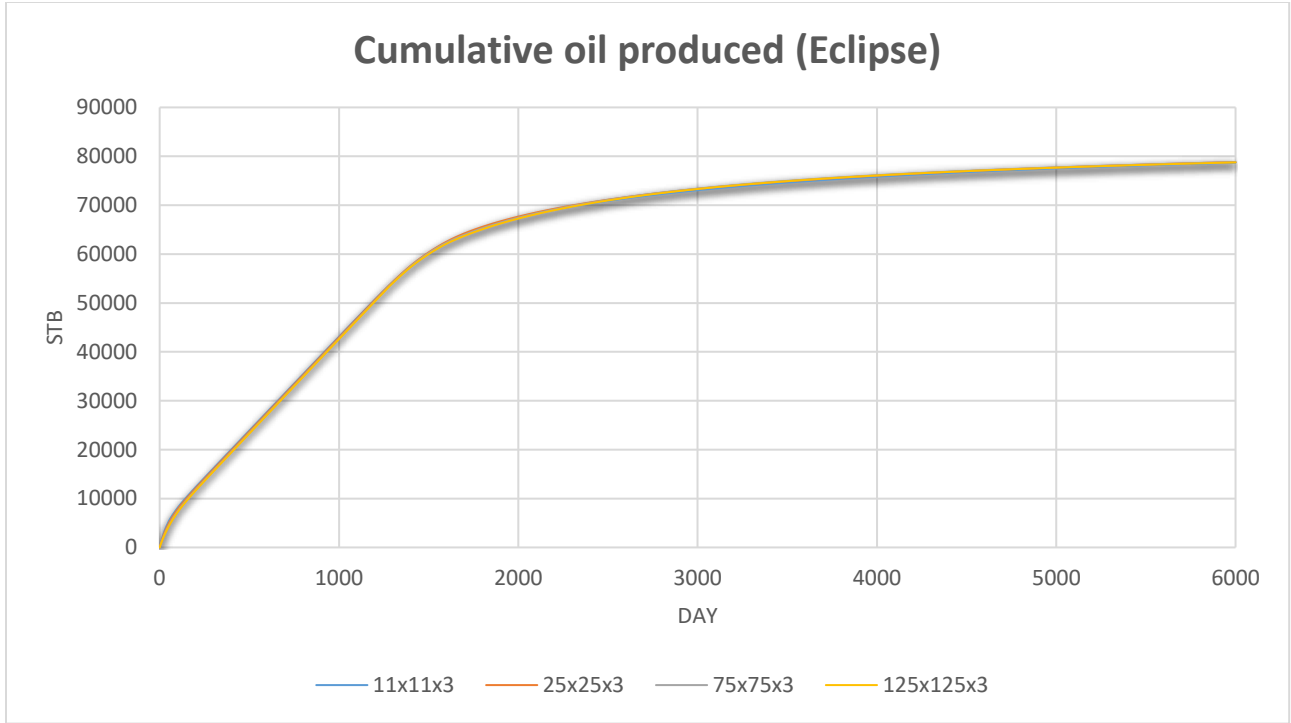


Figure 6.13 Cumulative oil produced in Eclipse convergence study runs

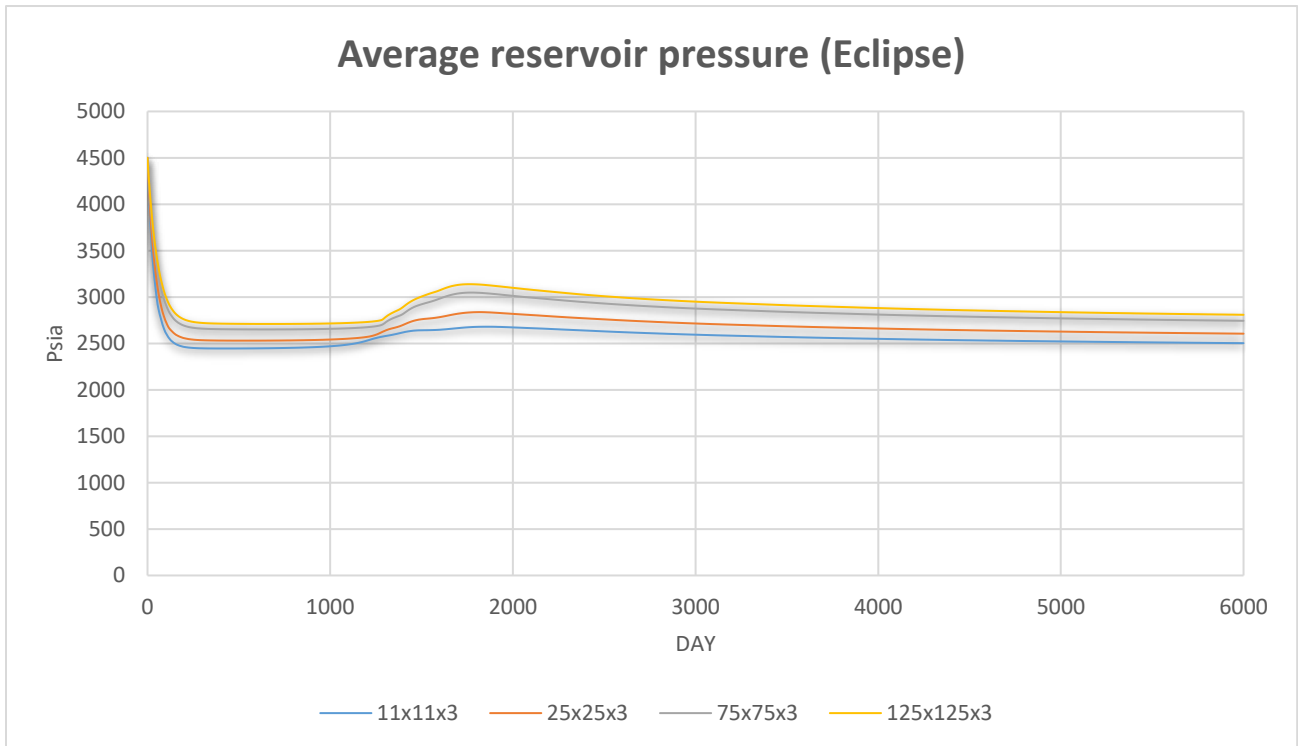


Figure 6.14 Average reservoir pressure in Eclipse convergence study runs

By observing the obtained results, only slight improvement was achieved by increasing the number of cells further than 75x75x3. But due to relatively short runtime of the larger 125x125x3 Model we will conclude that 125x125x3 Model converged, and take it as base model in future comparison.

6.3.2 tNavigator convergence study

Procedure was done in the same manner as for Eclipse simulator.

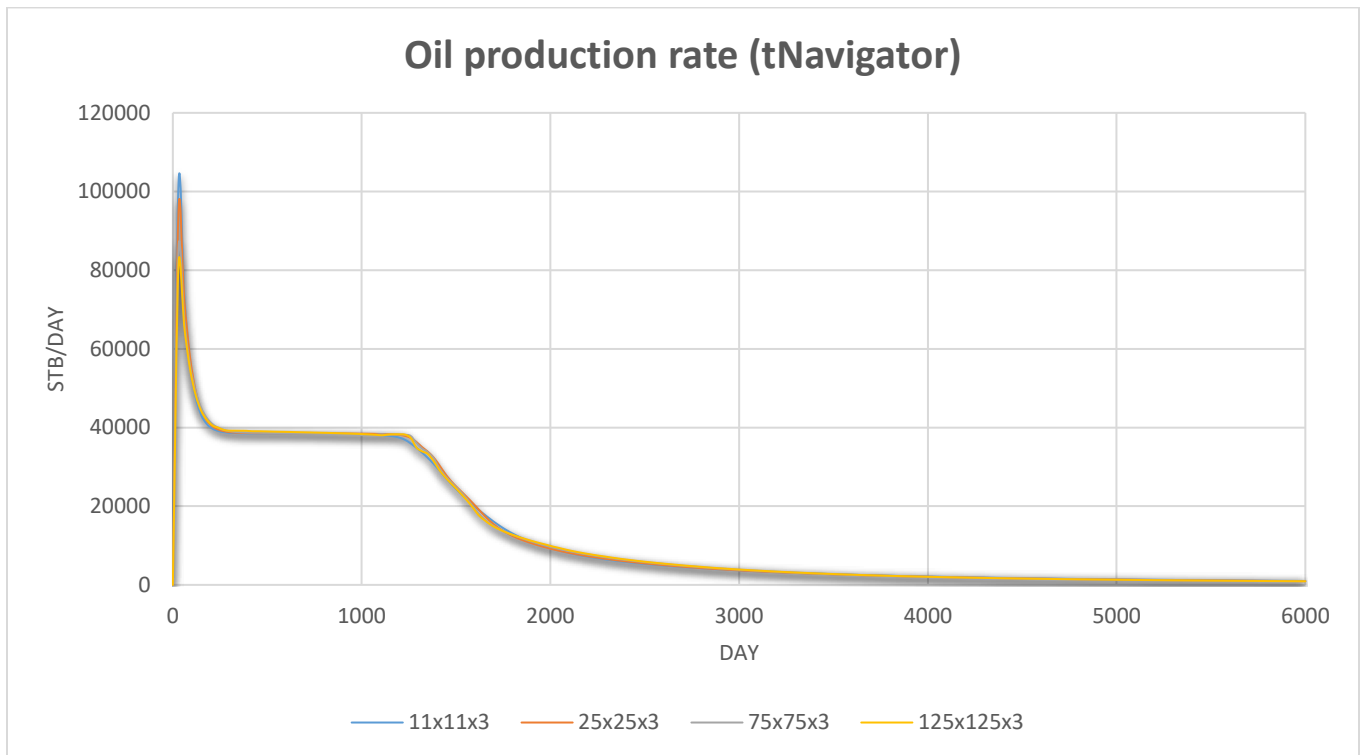


Figure 6.15 Oil production rate in tNavigator convergence study runs

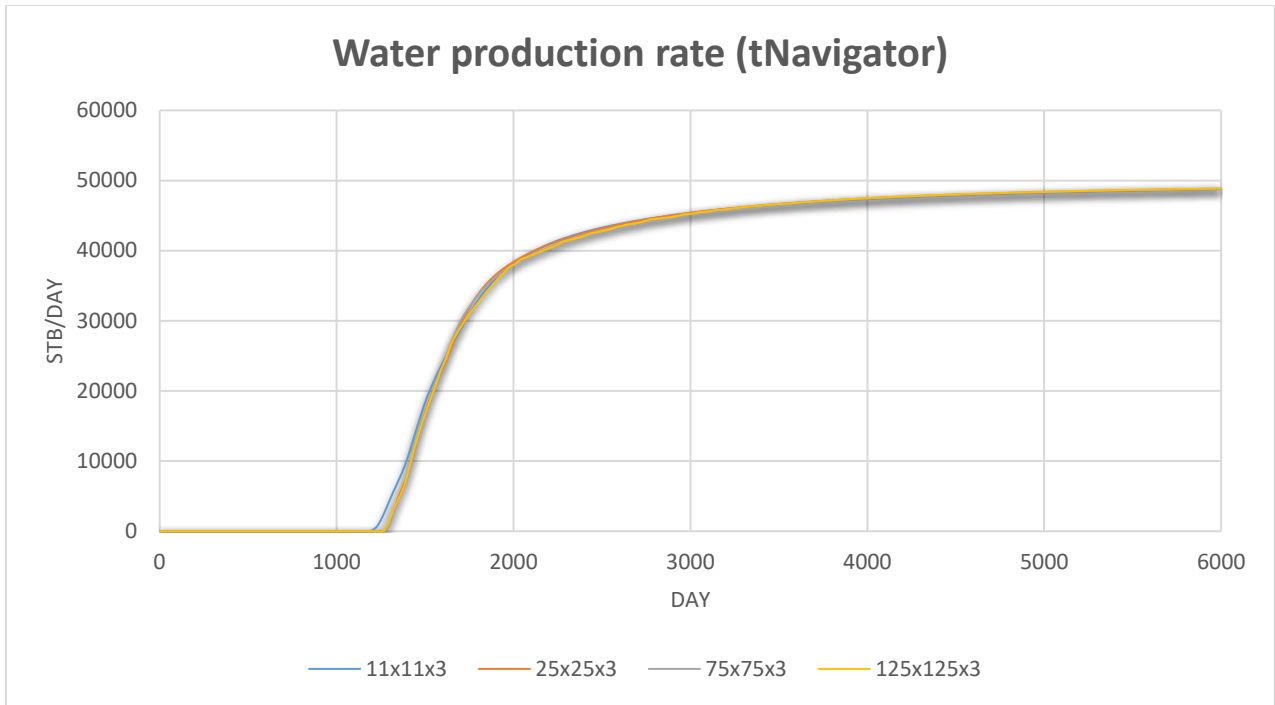


Figure 6.16 Water production rate in tNavigator convergence study runs

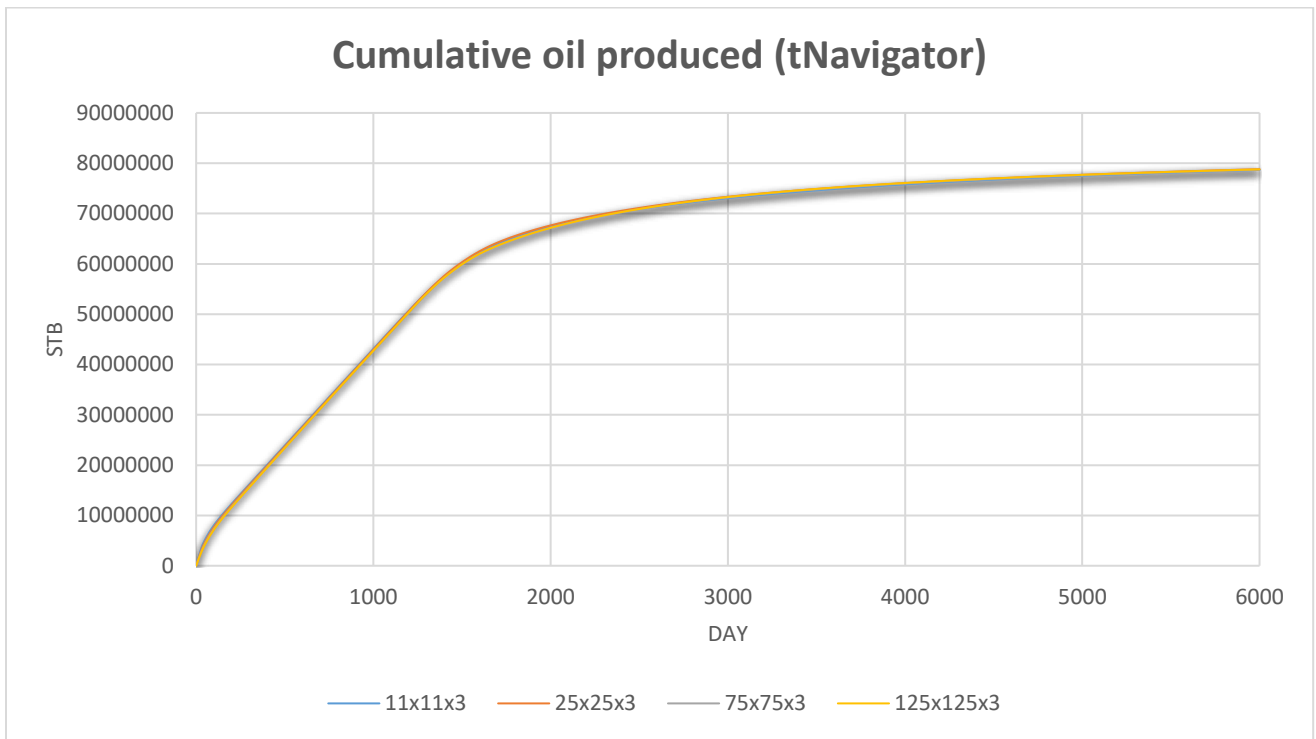


Figure 6.17 Cumulative oil produced in tNavigator convergence study runs

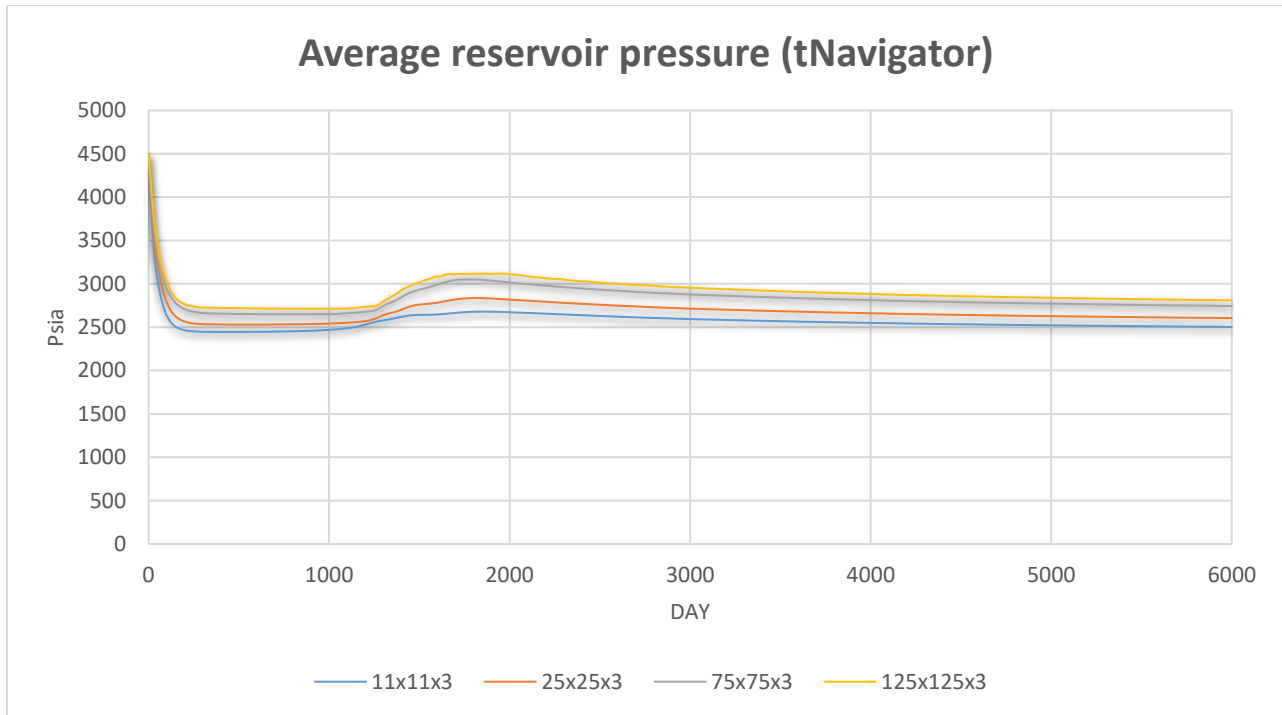


Figure 6.18 Average reservoir pressure in tNavigator convergence study runs

By observing obtained results we can realize that they are analog to trend observed in Eclipse convergence study. And as so we will conclude with the same sized model of 125x125x3 grid cell dimensions.

Regarding the physical interpretation of results, we can see that production plateau is reached quite fast and it lasts until water breakthrough. After that oil production rate starts to decay rapidly until the only flowing phase is water. All of this has an impact on reservoir average pressure, which is stable during production plateau until water breakthrough. Breakthrough causes gradual growth of hydrostatic pressure in the wellbore due to increased density of flowing fluid. That further causes average reservoir pressure to grow as well.

6.3.3 Comparison of converged models results

As we have decided which models are suitable for further use, and in both cases it will be model with 125x125x3 dimensions. In this chapter we will present comparison of those two models.

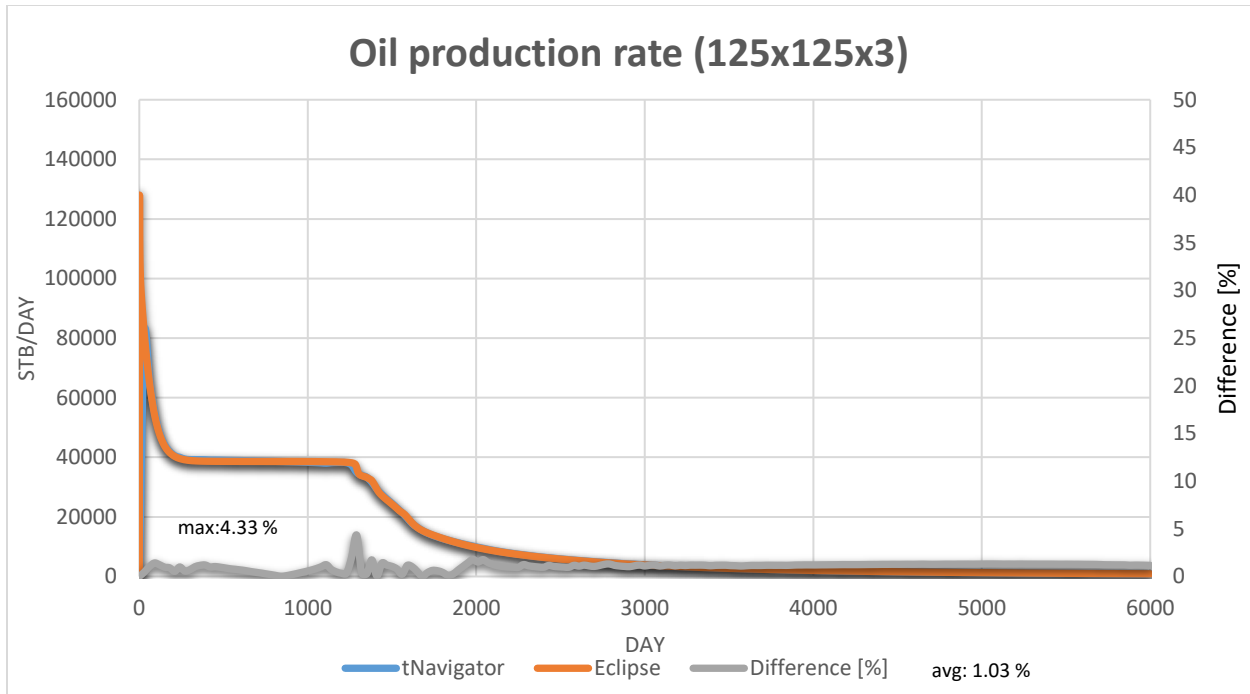


Figure 6.19 Oil production rate comparison

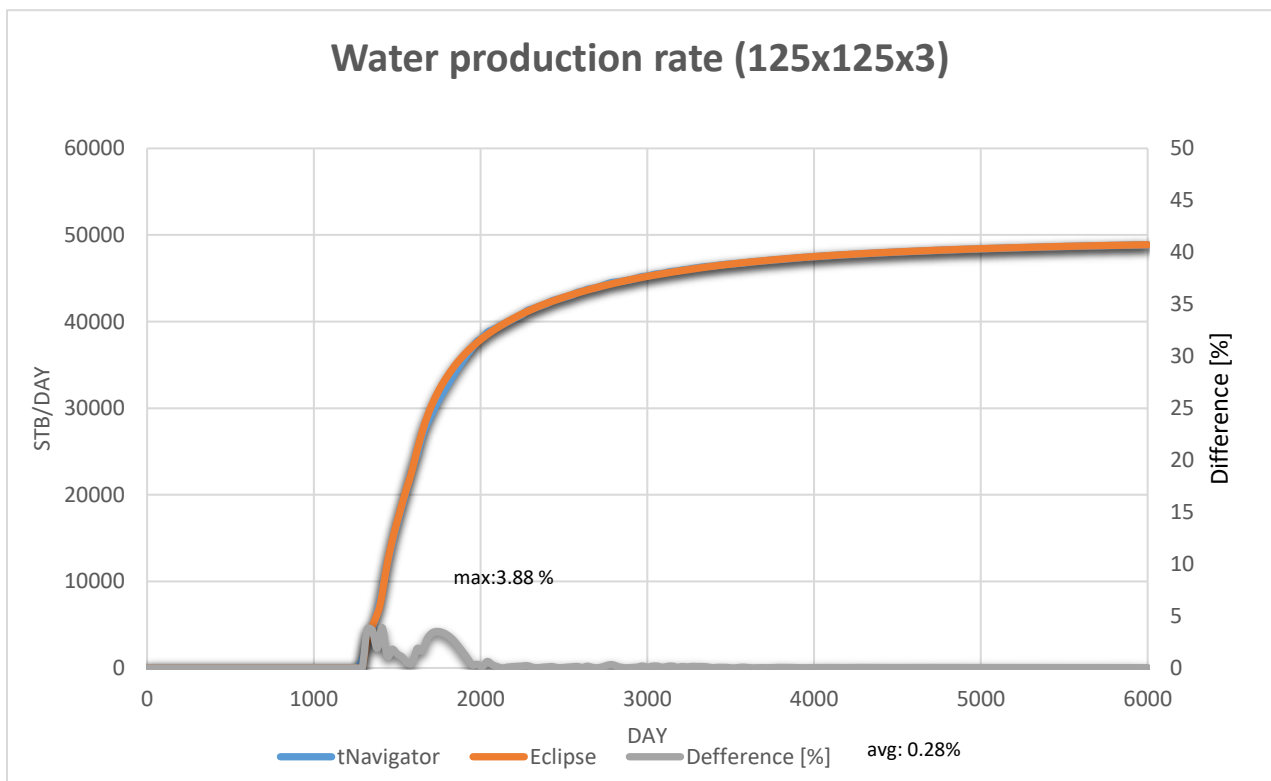


Figure 6.20 Water production rate comparison

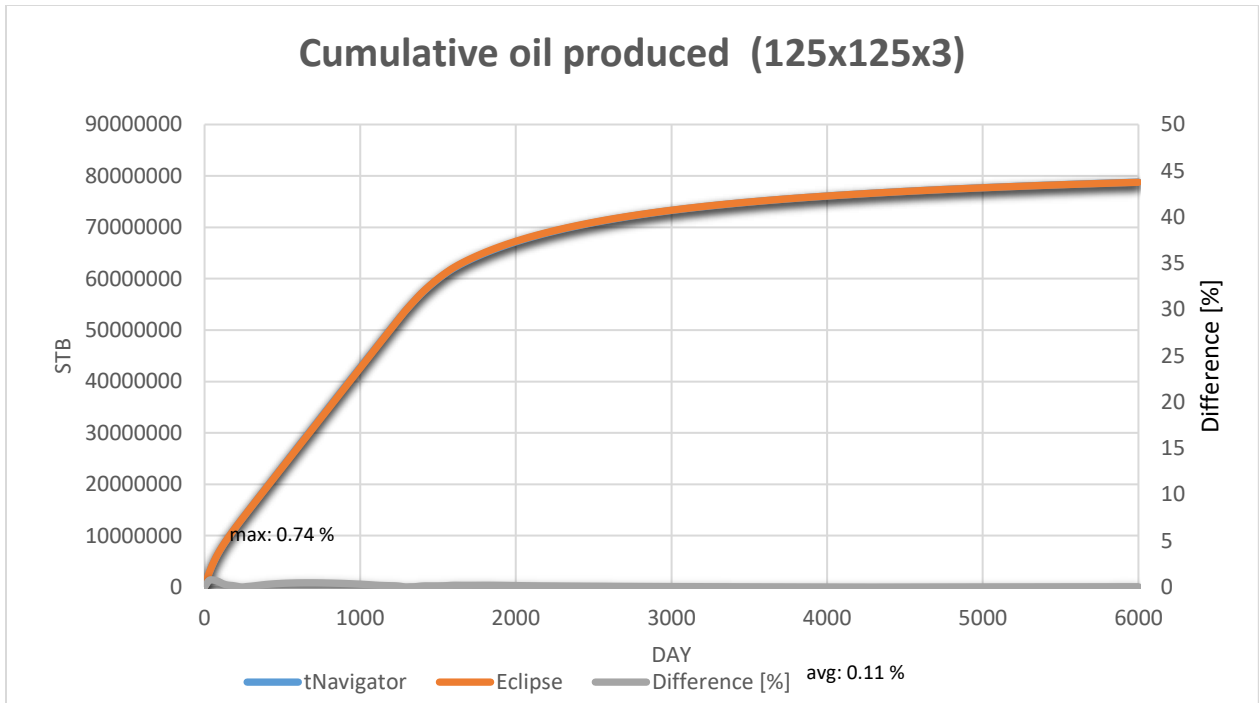


Figure 6.21 Cumulative oil produced comparison

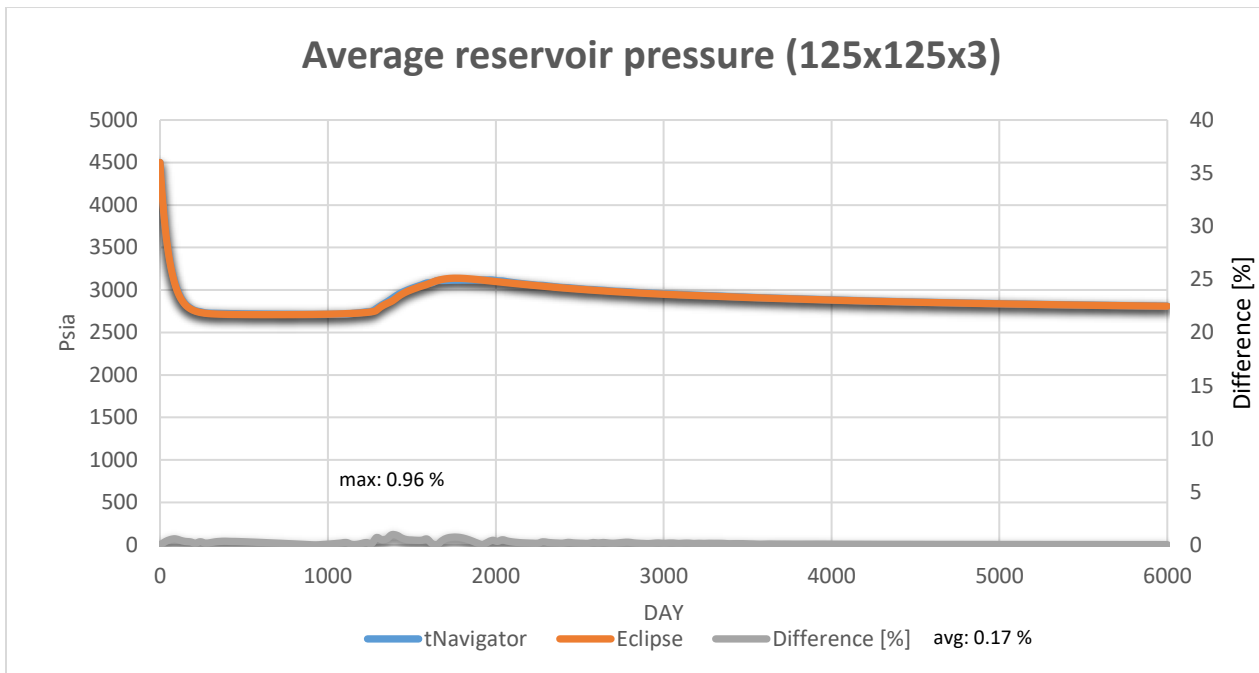


Figure 6.22 Average reservoir pressure comparison

As we can see from presented figures, results from both simulators are matching. With minor differences in output results ranging from 0 to 4.33% as the maximum value observed in oil production rate results (Figure 6.19) due to respective time step. The average difference takes the

maximum value of 1.03 % as well observed in oil production rate results, while lower average differences are observed on the rest of results. These differences are mainly coming from initialization steps or caused with sudden events such as water breakthrough.

6.4 Runtimes comparison

Earlier in this study we have secured fair comparison environment, by matching the output of both simulators on case of simple models. For which we believe the simulators should provide same output due to low complexity of models. As well one more important condition was that all runs were performed on same hardware, while all the background processes were terminated. This runtimes study is done by observing runtimes of models used in convergence study, all the times were measured in at least five consecutive runs of same model (Table 6.7), averaged and then presented on semi-log plot versus logarithmic value of number of cells for respective model (Figure 6.23).

Model	I	II	III	IV
X-direction number of cells	11	25	75	125
Y-direction number of cells	11	25	75	125
Z-direction number of cells	3	3	3	3
Total number of cells	363	1875	16875	46875

Table 6.8 Grid number of cells per model

CPU Runtime [s]							
Model I	Run I	Run II	Run III	Run IV	Run V	Average runtime	Time steps
Eclipse	0.66	0.67	0.45	0.64	0.48	0.58	206
tNavigator	0.1	0.1	0.1	0.1	0.1	0.1	205
Model II	Run I	Run II	Run III	Run IV	Run V	Average runtime	
Eclipse	1.12	1.67	2.14	1.5	1.16	1.518	211
tNavigator	0.2	0.2	0.2	0.2	0.2	0.2	205
Model III	Run I	Run II	Run III	Run IV	Run V	Average runtime	
Eclipse	14.84	14.95	14.91	14.92	15.03	14.93	266
tNavigator	14	15	16	16	16	15.4	211
Model III	Run I	Run II	Run III	Run IV	Run V	Average runtime	
Eclipse	75.83	75.81	75.58	75.62	75.67	75.702	302
tNavigator	67	67	67	67	67	67	232

Table 6.9 Observed runtimes

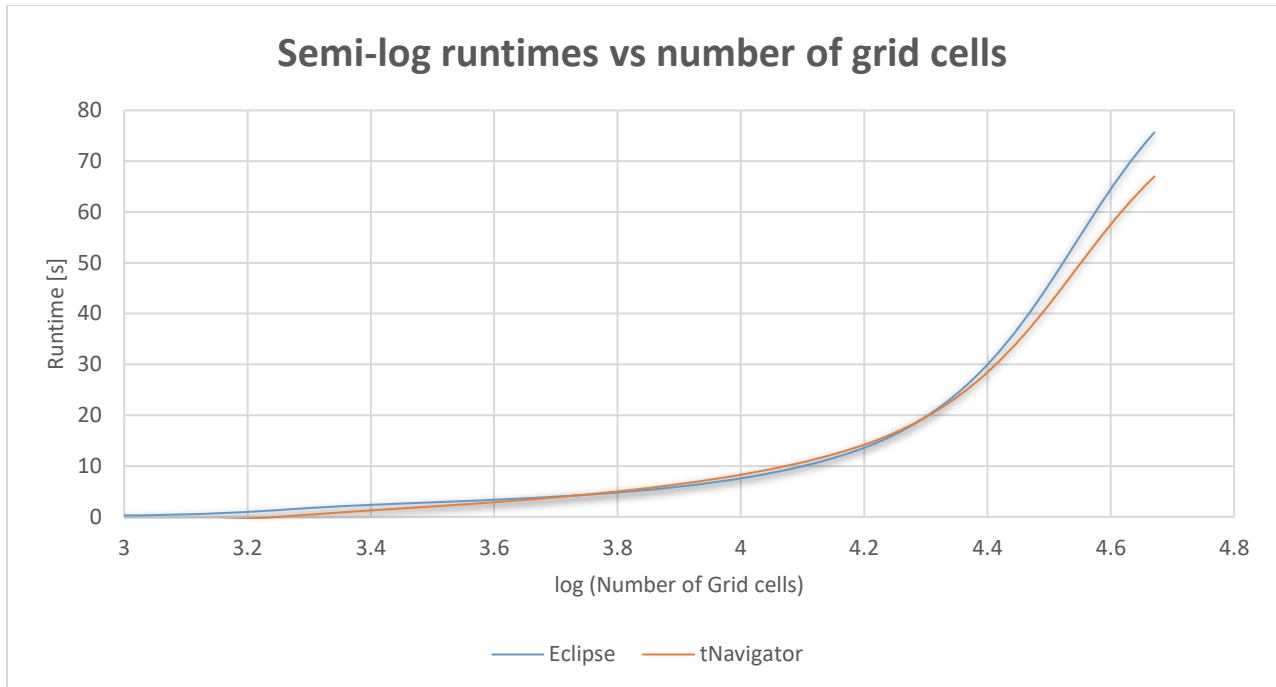


Figure 6.23 Runtimes comparison

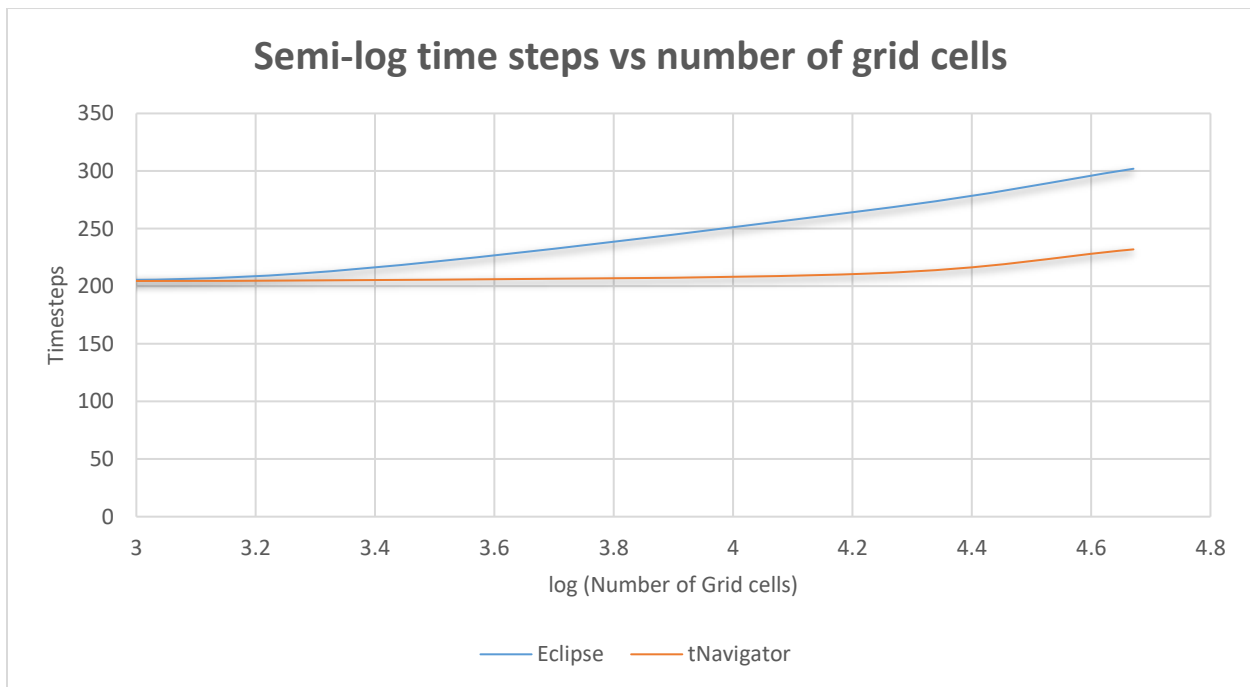


Figure 6.24 Time steps comparison

As we can see from obtained results, tNavigator reservoir simulator has less steep growth of runtimes as model complexity increases. This is first indicator of more efficient and faster performance. As well if we take into account number of time steps needed to execute

calculations, we can see that Eclipse reservoir simulator needs significantly more time steps. That can be taken as second indicator of efficiency, due to fact that simulator when unable to converge it is forced to reduce the time step size (increase number of time steps). And that directly affects the runtime of simulation.

7. SPE 9 Model

The model from the SPE-29110 paper is an extended test for three-phase three-dimensional Black-Oil modeling technique. The model involves oil production from a dipping initially undersaturated reservoir. There are 9000 grid blocks in total (rectilinear grid: 24*25*15). The permeability distribution is heterogeneous whereas the porosity distribution is homogeneous in every layer. The dip angle is 10 degrees. The oil-water capillary pressure is exposed to rapid variations under small saturation changes. There are 25 producers and a single water injector which is completed below oil-water contact. Production wells are constrained with maximal oil production of 1500 bbl/day and 1000psi BHP during first 5 time steps (300 days), after that the oil production rate is reduced to 100bbl/day for single time step (60 days) and then increased back to starting value of 1500 bbl/day. The Injection well is rate controlled with value of 5000 bbl/day. (Killough, 1995, January)

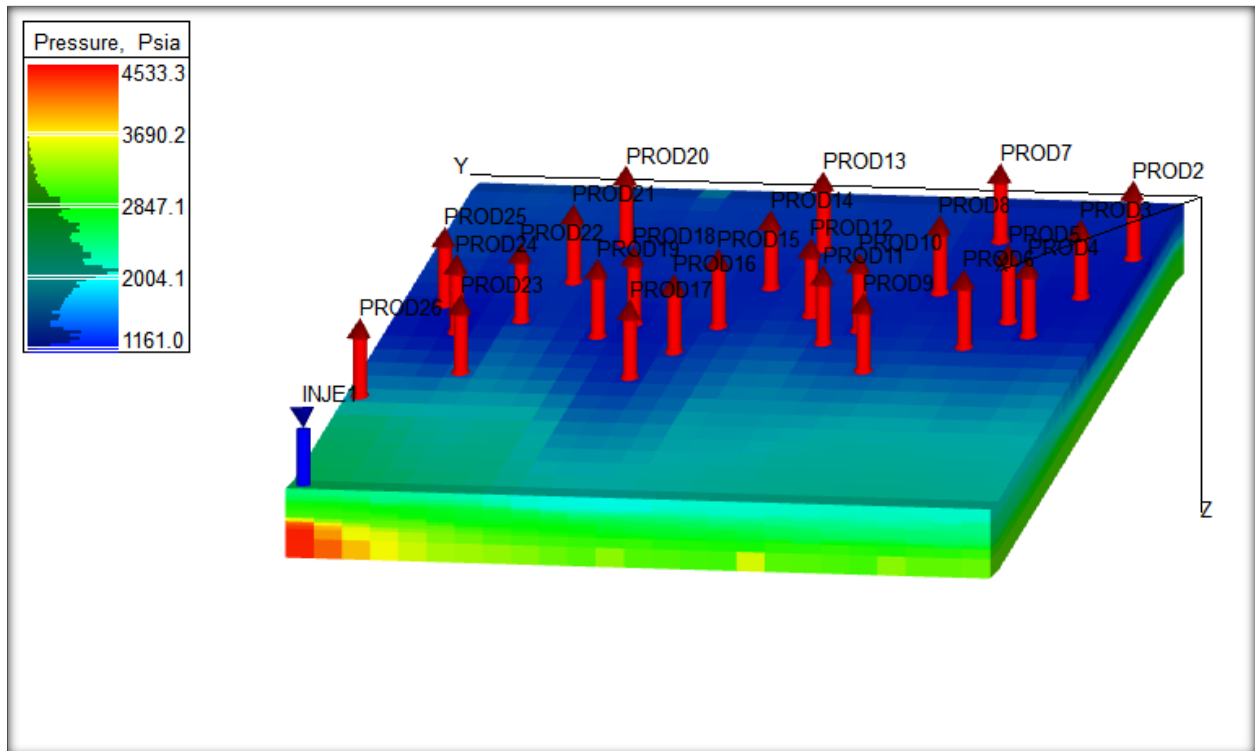


Figure 7.1 Model in 3D view (SPE 9)

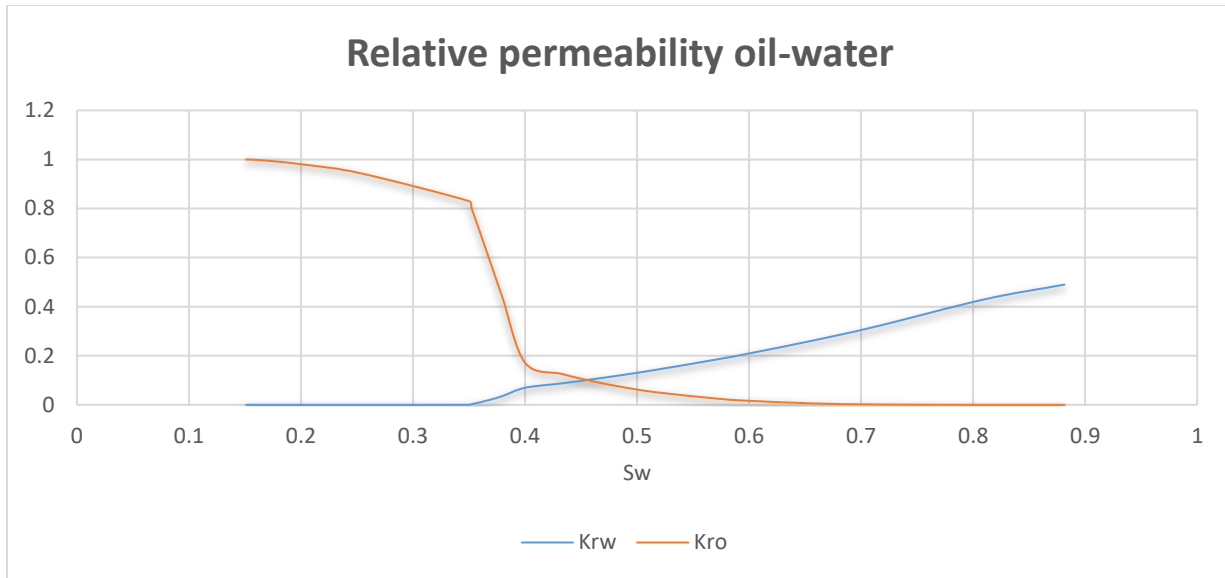


Figure 7.2 Relative permeability (SPE 9)

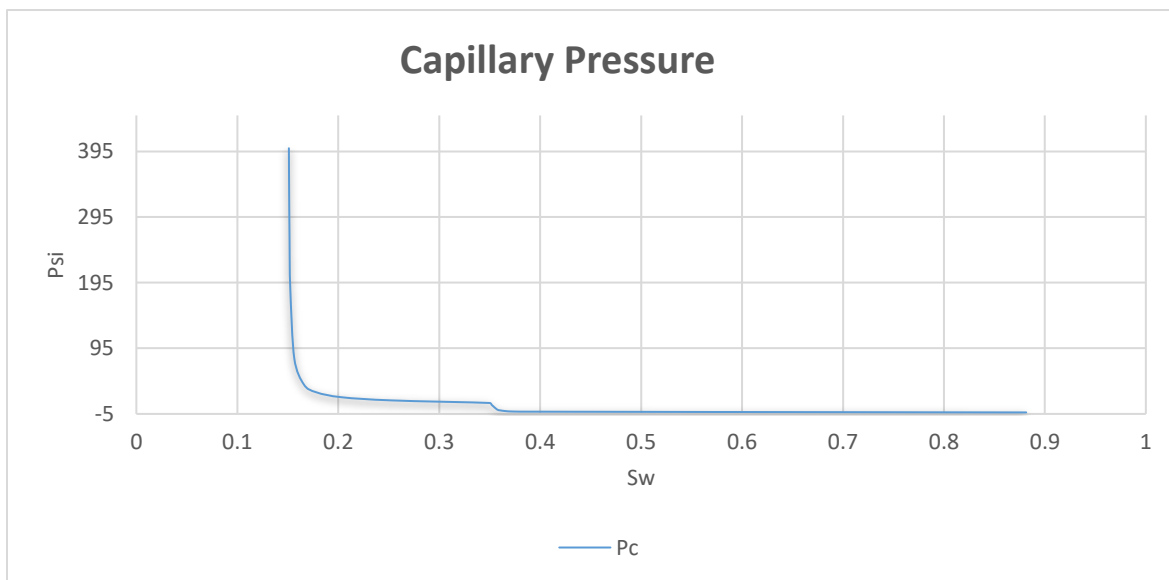


Figure 7.3 Capillary pressure (SPE 9)

Pressure	FVF, rb/stb	GOR, Mscf/stb	Viscosity, cP
14.7	1	0	1.2
400	1.01	0.165	1.17
800	1.02	0.335	1.14
1200	1.03	0.5	1.11
1600	1.05	0.665	1.08
2000	1.06	0.828	1.06
2400	1.07	0.985	1.03
2800	1.08	1.13	1
3200	1.09	1.27	0.98
3600	1.11	1.39	0.95
4000	1.12	1.5	0.94
5000	1.11	1.5	0.94

Table 7.1 PVTO (SPE 9)

Oil, lbm/ft3	Water, lbm/ft3	Gas, lbm/ft3
44.98	63.01	0.0702

Table 7.2 Densities (SPE 9)

SPE 9 model will be used as final comparison between these two simulators. The emphasis will be in oil production rate and reservoir average pressure.

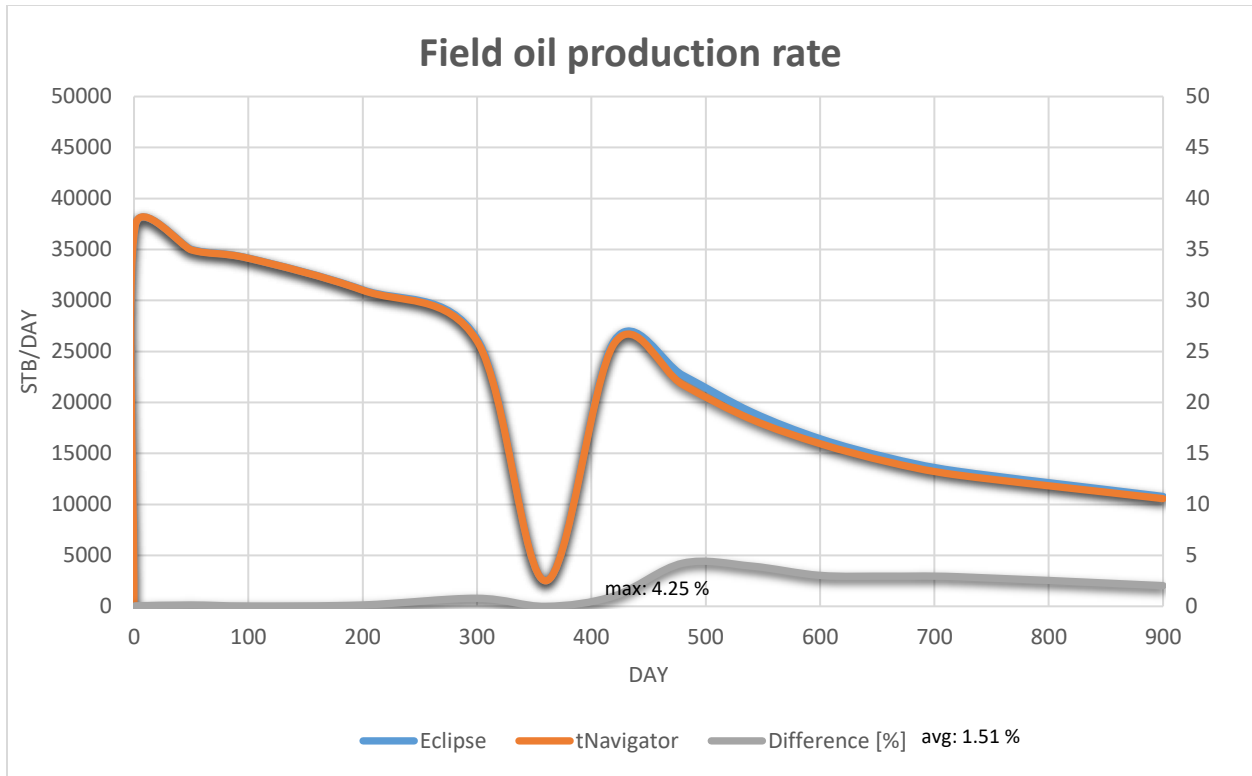


Figure 7.4 Field oil production rate (SPE 9)

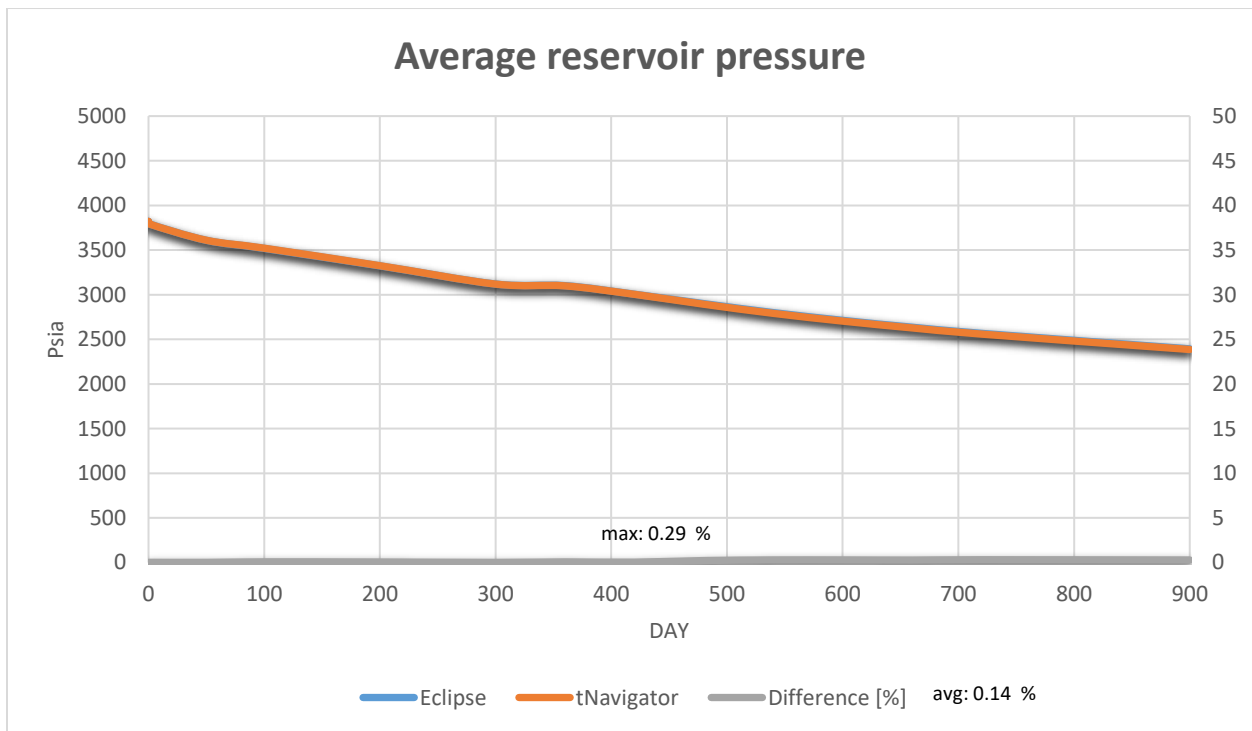


Figure 7.5 Average reservoir pressure (SPE 9)

As it can be seen from output results, both simulators are providing quite similar results. With slight difference appearing right after the disturbance introduced with temporary reduction of production rate. Main purpose of SPE 9 model was to study how simulators are handling abrupt changes in time steps sizes while running complex model like this.

Time step	Model defined	Eclipse	tNavigator
1	1	1	1
2	50	3	50
3	100	6	100
4	200	12	200
5	300	29	300
6	360	50	360
7	420	75	420
8	480	100	480
9	540	115	540
10	600	140	600
11	660	170	660
12	720	200	720
13	900	250	900
14		300	
15		320	
16		340	
17		360	
18		420	
19		480	
20		510	
21		540	
22		600	
23		660	
24		720	
25		750	
26		810	
27		855	
28		900	

Table 7.3 Time steps (SPE 9)

As it can be seen Eclipse reservoir simulator fails to execute time step sizes defined by the model. And instead of finishing the run in thirteen time steps it takes additional 15 time steps. This is a strong indicator of solver efficiency used by the respective simulator.

8. Conclusion

Under this study we have executed all the steps explained in strategy section. From establishing fair comparison environment by matching results of simple models, to running convergence study by increasing complexity of models and monitoring respective runtimes. As a final comparison we had SPE 9 model.

By taking into account all observed results, we could say that both simulators are providing quite similar output results (variations of max 5% were observed). Regarding runtime of simulations, we have observed quite similar runtimes for low complexity models, while for more complex models we start to notice mismatch in runtimes. And if trends of runtimes observed extend in the same fashion, we can make a conclusion that tNavigator is faster and deals better with models of higher complexity.

As well in the final study of SPE 9 model runs, we could see that tNavigator manages to deal with demanding time steps, while Eclipse fails to do so and is forced to break time steps. That results in higher CPU runtimes. If we take this as an indicator of solver efficiency and capability to converge even with larger time steps, then we could definitely say that tNavigator simulator is more efficient.

Regarding the work itself in both of these simulators, my personal impression is that tNavigator is quite user-friendly compared to Eclipse, and provides very useful feature to monitor your calculations real time during every time step. It's strength lays in parallel computing and full utilization of computer hardware, that practically means that the better computer we use more efficient it becomes compared to old industry standard software such as Eclipse.

9. Bibliography

- [1] Chen, Z. (2001). Formulations and Numerical Methods of the Black Oil Model in Porous Media. *SIAM Journal on Numerical Analysis*, 489-514.
- [2] Dake, L. P. (2013). *The practice of reservoir engineering*.
- [3] Ertekin, T. A.-K. (2001). *Basic applied reservoir simulation*.
- [4] Ewing, R. E. (1983). *The mathematics of reservoir simulation*. Society for Industrial and Applied Mathematics.
- [5] Killough, J. E. (1995, January). Ninth SPE comparative solution project: a reexamination of black-oil simulation. *SPE Reservoir Simulation Symposium*.
- [6] Pengbo Lu, B. B. (2011). An Adaptive Newton's Method for Reservoir Simulation. *SPE Reservoir Simulation Symposium*.
- [7] *Reservoir Engineering*. (2013). Heriot Watt University .
- [8] Schlumberger. (2010). *ECLIPSE (ECLIPSE* reservoir simulation software Version 2010.1) Reference Manual*.